Article

Cell

Drastic Genome Reduction in an Herbivore's Pectinolytic Symbiont

Graphical Abstract

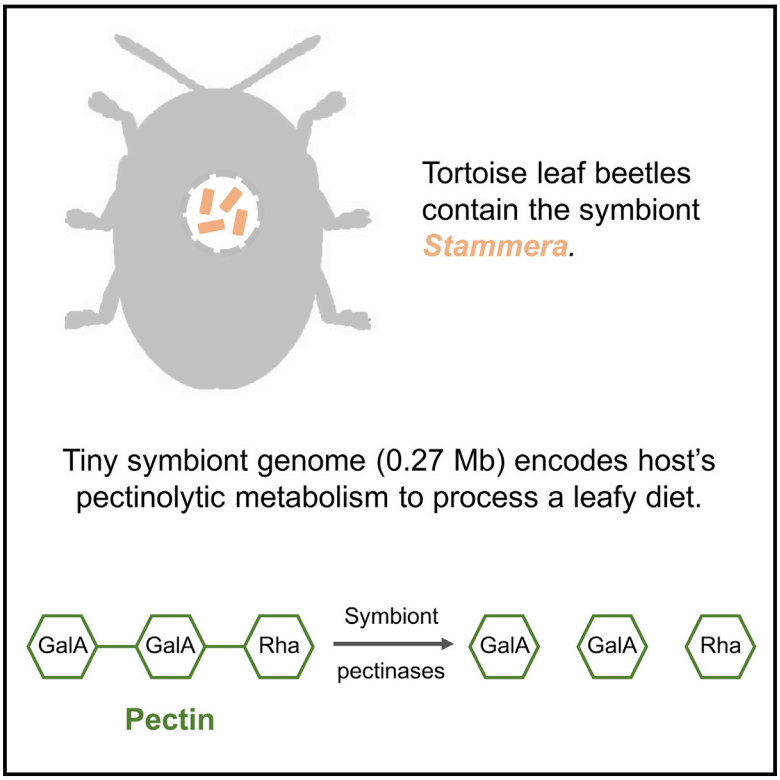

Authors

Hassan Salem, Eugen Bauer, Roy Kirsch, ..., Heiko Vogel, Takema Fukatsu, Martin Kaltenpoth

Correspondence

hssalem@emory.edu

In Brief

A proteobacterial symbiont with the smallest known genome of an extracellular bacterium provides its host beetle with key enzymes to break down pectin in plant-based food, giving a striking example of symbiosis and evolutionary adaptation.

Highlights

- Symbiosis is a strategy for an herbivore to gain pectinolytic metabolic enzymes
- *Stammera* has the smallest genome of any known organism not living within a host cell
- Specialized structures on the beetle house the symbiont and ensure vertical transfer
- Symbiont acquisition likely relaxed selection for the host to endogenously maintain pectinases

Salem et al., 2017, Cell *171*, 1520–1531
December 14, 2017
https://doi.org/10.1016/j.cell.2017.10.029

CellPress

Cell

Article

Drastic Genome Reduction in an Herbivore's Pectinolytic Symbiont

Hassan Salem,[1,2,10,*] Eugen Bauer,[3,9] Roy Kirsch,[4,9] Aileen Berasategui,[1,2,5] Michael Cripps,[6] Benjamin Weiss,[1,7] Ryuichi Koga,[8] Kayoko Fukumori,[8] Heiko Vogel,[4] Takema Fukatsu,[8] and Martin Kaltenpoth[1,7]

[1]Insect Symbiosis Research Group, Max Planck Institute for Chemical Ecology, Jena 07745, Germany
[2]Department of Biology, Emory University, Atlanta, GA 30320, USA
[3]Luxembourg Centre for Systems Biomedicine, University of Luxembourg, Esch-sur-Alzette 4365, Luxembourg
[4]Department of Entomology, Max Planck Institute for Chemical Ecology, Jena 07745, Germany
[5]Department of Biochemistry, Max Planck Institute for Chemical Ecology, Jena 07745, Germany
[6]AgResearch, Lincoln Research Centre, Lincoln 7608, New Zealand
[7]Department of Evolutionary Ecology, Johannes Gutenberg University, Mainz 55128, Germany
[8]National Institute for Advanced Industrial Science and Technology, Tsukuba 305-8566, Japan
[9]These authors contributed equally
[10]Lead Contact
*Correspondence: hssalem@emory.edu
https://doi.org/10.1016/j.cell.2017.10.029

SUMMARY

Pectin, an integral component of the plant cell wall, is a recalcitrant substrate against enzymatic challenges by most animals. In characterizing the source of a leaf beetle's (*Cassida rubiginosa*) pectin-degrading phenotype, we demonstrate its dependency on an extracellular bacterium housed in specialized organs connected to the foregut. Despite possessing the smallest genome (0.27 Mb) of any organism not subsisting within a host cell, the symbiont nonetheless retained a functional pectinolytic metabolism targeting the polysaccharide's two most abundant classes: homogalacturonan and rhamnogalacturonan I. Comparative transcriptomics revealed pectinase expression to be enriched in the symbiotic organs, consistent with enzymatic buildup in these structures following immunostaining with pectinase-targeting antibodies. Symbiont elimination results in a drastically reduced host survivorship and a diminished capacity to degrade pectin. Collectively, our findings highlight symbiosis as a strategy for an herbivore to metabolize one of nature's most complex polysaccharides and a universal component of plant tissues.

INTRODUCTION

The polysaccharide networks that comprise the cell walls of plants serve as the largest reservoir of organic carbon on Earth (Rose, 2003). Pectin, the most complex of these polymers (Mohnen, 2008), is instrumental towards ensuring plant cellular integrity, adhesion, and signal transduction and constitutes a formidable barrier preventing parasites and pathogens from entering the cytosol (Underwood, 2012).

While pectin classes vary considerably in their degree of methylation and propensity to form side chains, their backbones follow one of two polysaccharidic sequences: a galacturonic acid homopolymer (e.g., homogalacturonan, xylogalacturonan) or a galacturonic acid-rhamnose heteropolymer (rhamnogalacturonan I) (Burton et al., 2010). Together, homogalacturonan and rhamnogalacturonan I represent the most abundant glycan classes within plant tissue (~65% and ~30%, respectively) (Voragen et al., 2009; Rose, 2003), overwhelmingly contributing to a pectin matrix where cellulose and hemicellulose are embedded to provide rigidity to the primary cell wall.

Given the carbon- and energy-rich composition of plant cell walls, phytophagous organisms have evolved a range of metabolic adaptations aimed at converting the composite fibers into digestible mono- or oligosaccharides through the production of plant cell wall degrading enzymes (PCWDEs) (Alfano and Collmer, 1996). Pectin is most commonly monomerized by enzymes such as polygalacturonases (PGs), pectate lyases (PLs), and pectin methylesterases (PMEs) (Gilbert, 2010). The vast majority of pectinolytic enzymes are annotated in microbial genomes, typically in the form of glycoside hydrolases capable of breaching the polysaccharide's glycosidic bonds through single or double displacement mechanisms (Jayani et al., 2005; Rye and Withers, 2000). These enzymes are elemental to the metabolism of phytopathogens, exemplified by their enrichment across genomes belonging to bacterial and fungal taxa exploiting this ecological niche (Abbott and Boraston, 2008; Sprockett et al., 2011), as well as their preferential expression during the early stages of infecting a plant cell (De Lorenzo and Ferrari, 2002; Blackman et al., 2015).

While animals were thought to be categorically deficient in their repertoire of pectinolytic enzymes, recent efforts have annotated and functionally characterized a range of pectinase-coding genes in genomes of herbivorous arthropods following horizontal acquisition from microbes (Calderón-Cortés et al., 2012; Boto, 2014; Wybouw et al., 2016). Notably,

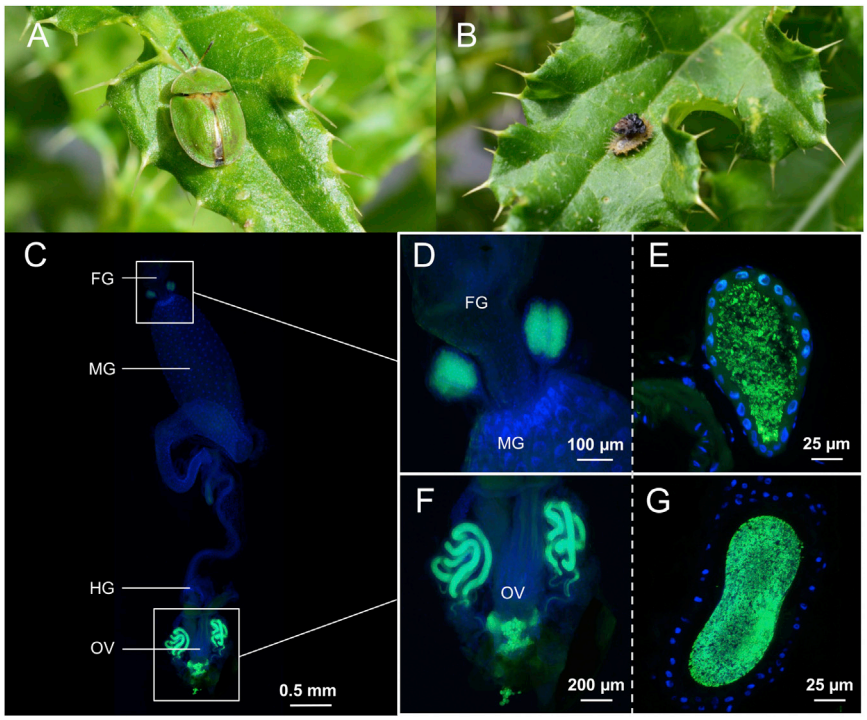

Figure 1. Localization of *Stammera* within the Tortoise Leaf Beetle

(A and B) An adult (A) and larva (B) of *Cassida rubiginosa*.

(C) Whole-mount fluorescence *in situ* hybridization (FISH) targeting 16S rRNA of *Stammera* (green) within an adult female beetle's digestive and reproductive organs. DAPI (blue) was used for counterstaining.

(D and E) Whole-mount (D) and cross section (E) of the foregut-associated symbiotic organs.

(F and G) Whole-mount (F) and cross section (G) of the symbiont reservoirs associated with the ovaries. FG, foregut; MG, midgut; HG, hindgut; OV, ovaries. Scale bars are included for reference.

the integration of bacterial pectinase genes by stick insects preceded the diversification and ecological expansion of the suborder (Shelomi et al., 2016). Similarly, weevils (Curculionoidea), long-horn beetles, and leaf beetles (Chrysomeloidea), were found to share a single origin of PGs, which can be attributed to an ascomycete fungus-to-beetle transfer nearly 200 million years ago (Kirsch et al., 2014, 2016). Such findings, among others (Danchin et al., 2010), point toward the consequential impact of horizontal gene transfer of pectinase-coding genes and the evolution of herbivory in arthropods (Wybouw et al., 2016).

As an alternative to horizontally acquiring genes coding for essential metabolites or enzymes, symbioses have aptly been demonstrated to endow animals with adaptations facilitating their radiation into novel environments (Moran, 2007). The annotation of pectinase-coding genes in metagenomic and transcriptomic descriptions of complex gut microbial communities in bees (Engel et al., 2012), humans (Martens et al., 2011), and various ruminants (Pope et al., 2012; Patel et al., 2014) revealed a framework for how animals can process pectin in the absence of horizontal gene transfer events. In revisiting 80-year-old histological descriptions (Stammer, 1936), we extend this narrative by detailing a highly streamlined symbiosis defined by a microbe's ability to confer a pectinolytic phenotype to its insect host. Specifically, we demonstrate that the novel bacterial symbiont "*Candidatus* Stammera capleta" is obligately beneficial to the tortoise beetle *Cassida rubiginosa*, and—despite an unusually diminutive genome for an extracellular microbe—is responsible for its host's ability to break down pectin, a vital contribution considering the metabolic and nutritional requirements of an insect folivore.

RESULTS

Stammera, a Symbiont of Tortoise Leaf Beetles

Molecular characterization of *C. rubiginosa*'s bacterial associates using amplicon pyrosequencing of the 16S rRNA gene revealed a community dominated by *Wolbachia* sp. (69%) and *Stammera* (31%) (Figure S1) (NCBI SRA: SRP119423). Subsequent diagnostic PCRs indicated that while *Stammera* is universally present (100%) across four *C. rubiginosa* populations spanning New Zealand, the United States, Germany, and Japan (Table S1), the distribution of *Wolbachia* appeared less uniform (44%), suggesting a more facultative partnership with the leaf beetle (Table S1). Based on complete 16S rRNA sequences, phylogenetic analysis resulted in the monophyletic placement of *Stammera* alongside other obligate insect symbionts within the γ-proteobacteria class, including *Buchnera* of aphids and *Blochmannia* of carpenter ants (Figure S2).

Localization of *Stammera* within Its Beetle Host

In line with earlier histological descriptions involving adults and larvae within the Cassidinae (Stammer, 1936), whole-mount fluorescence *in situ* hybridization (FISH) of *C. rubiginosa* confirmed *Stammera*'s localization to be restricted to a pair of sac-like structures connected to the foregut, as well as, in females, two glandular reservoirs opening into the lower third of the insect's vagina (Figure 1). For the latter, each reservoir is composed of three finger-like tubules connected to the ovipositor by a delicate passage and is densely populated by the symbionts, likely to facilitate transmission as evidenced by the subsequent packaging of microbes at the intersection of the passages and the vagina (Figure 1F).

To further localize *Stammera* within the symbiotic organs associated with the foregut as well as the female reproductive tract, we employed fluorescence *in situ* hybridization (FISH) using semi-thin (2 μm) cross sections of both structures (Figures 1E and 1G). Despite discrete clusters within both organs, the symbionts were found to subsist in a matrix beyond the cellular boundaries of their host, indicative of a clear

extracellular localization within highly specialized structures bearing semblance to bacteriocyte-based partnerships.

The Egg Caplet as a Vehicle for Symbiont Transmission

In outlining *Stammera*'s transmission cycle within its beetle host, we utilized FISH and 3D reconstructions to visualize symbiont localization following oviposition. The eggs, deposited in clutches of 3–9 per ootheca (Figure 2A), are singularly topped with a distinct cap-like structure at the anterior pole (Figure 2B); one hypothesized to contribute toward the vertical transmission of the symbionts following ingestion by an emerging larva (Stammer, 1936). Three-dimensional reconstructions of the egg caplets revealed that the structures enclose 20–30 spheres (Figure 2C) resembling those observed at the intersection of the passage connecting symbiont-harboring accessory glands and the vagina (Figure 1F). By applying FISH on semithin cross sections of the eggs, we demonstrate that the spheres are densely populated with *Stammera* (Figures 2D and 2E).

QPCR assays targeting *Stammera*'s 16S rRNA gene were used to quantify symbiont population dynamics across different developmental host stages, including eggs, larvae (1st, 3rd, 5th instars), pupae, and adults (pre- and post-diapause) (Figure 2F). Reproductively active, post-diapause females harbored on average 2.8 million *Stammera* cells, 0.28% of which (7.7×10^4 cells) were subsequently packaged into individual egg caplets. While *Stammera*'s population gradually recovers throughout larval development, a second, more drastic reduction in population size afflicts the microbes as the host undergoes metamorphosis (Figure 2F). Specifically, of the 8.9×10^5 *Stammera* cells quantified within 5th instar larvae, only ~600 cells could be detected during the pupal stage. In quantifying the total population bottleneck affecting *Stammera* vis-à-vis egg caplet transmission and metamorphosis, we estimate that only 0.02% [$(600 \div 2.8 \times 10^6) \times (100)$] of the starting symbiont population is available to an emerging, pre-diapause adult beetle. Because genome polyploidy is described for some bacterial endosymbionts (Komaki and Ishikawa, 1999, 2000), we note that symbiont population descriptions based on gene quantifications may reflect overestimates, as previously discussed by Hosokawa et al. (2007).

A Host-Beneficial Symbiosis

To assess *Stammera*'s impact on host survivorship and development, we generated symbiont-free (aposymbiotic) larvae by piercing their egg caplets prior to emergence (Movie S1) followed by sterilizing the eggs' anterior poles using 95% ethanol. Success of the egg surface sterilization procedure was confirmed by *Stammera*-specific diagnostic PCRs (Table S2). Survival rates of aposymbiotic individuals were then compared to two symbiont-containing groups (Figure 2G): larvae from untreated eggs, as well as larvae from eggs whose caplets were sterilized but not punctured. Symbiont-free larvae exhibited significantly lower survivorship to adulthood relative to larvae whose eggs were left untreated (Figure 2G; $p = 0.044$, Kaplan-Meier, Tarone-Ware test), as well as larvae whose caplets were sterilized but not punctured (Figure 2G; $p = 0.043$, Kaplan-Meier, Tarone-Ware test), confirming *Stammera* as a beneficial symbiont to the tortoise leaf beetle. Both symbiont-containing treatments exhibited similar survivorship rates (Figure 2G; $p = 0.924$, Kaplan-Meier, Tarone-Ware test), demonstrating that the adverse effects recorded for aposymbiotic larvae were not an immediate consequence of ethanol exposure.

Symbiont Genome Drastically Streamlined to Break down Pectin

General genomic features of *Stammera* (Figure 3A; GenBank: CP024013) were strikingly similar to those belonging to intracellularly localized endosymbionts (Figures 3B–3D; Table S3). Specifically, *Stammera*'s genome consists of a circular 271,175 bp chromosome with an 84.6% AT content (Figure 3A), encoding only 251 putative protein-coding open reading frames (ORFs) with an average size of 932 bp, resulting in a coding percentage of 89%. Of these, 233 were assigned to putative biological functions, whereas 18 matched hypothetical proteins of unknown function. A single ribosomal operon could be annotated with three structural ribosomal RNA genes (5S, 16S, 23S), as well as 29 tRNA genes assigning all 20 amino acids.

During gene prediction, it became apparent that many protein-coding regions were prematurely interrupted by putative stop codons. We noted through multiple protein alignments against sequences from other Proteobacteria that the stop codon UGA consistently appeared where tryptophan was expected to occur. While unusual, previous studies have reported that codons can acquire novel assignments. Specifically, the observation that UGA was reassigned to code for tryptophan instead of a stop codon is in line with alternative coding schemes recorded in several bacterial lineages with drastically reduced genomes (Yamao et al., 1985; McCutcheon et al., 2009), as well as in mitochondria (Sengupta et al., 2007). As such, genome annotation in this study was carried out using the NCBI genetic code 4 (TGA encoding tryptophan) as described by McCutcheon et al. (2009).

While retaining some genes necessary for basic cellular functions, including translation, replication, and energy conversion via glycolysis, we discovered that *Stammera*'s drastically reduced genome reflects an unusually deficient metabolic profile for a bacterium exhibiting an extracellular lifestyle (Figures 3C and 3D), in line with our assessment that it represents the smallest known genome of any organism not subsisting within a host cell. Notably, the symbiont's genome lacked the genes necessary for the Krebs cycle and flagellar motility; as well as long chain fatty acid, phospholipid, and purine biosynthesis.

Despite a close phylogenetic affiliation to many nutritional endosymbionts of insects (Figure S2), *Stammera* nonetheless lost the biosynthetic pathways underlying nutritional supplementation of essential nutrients (Figure 3D). Specifically, the symbiont lacks the metabolic capacity to produce all essential amino acids and B vitamins. Strikingly, but complementary to its host's feeding ecology, is the enrichment of a set of genes involved in the regulation, production, and export of two pectinases targeting the backbones of the most abundant pectic classes: homogalacturonan and rhamnogalacturonan I (Figures 3E and 3F). This includes a PG belonging to the glycoside hydrolase family 28 predicted to cleave the 1,4-linkages of the homogalacturonan polymer, as well as a rhamnogalacturonan lyase (RL) belonging to the polysaccharide lyase 4 family predicted to degrade

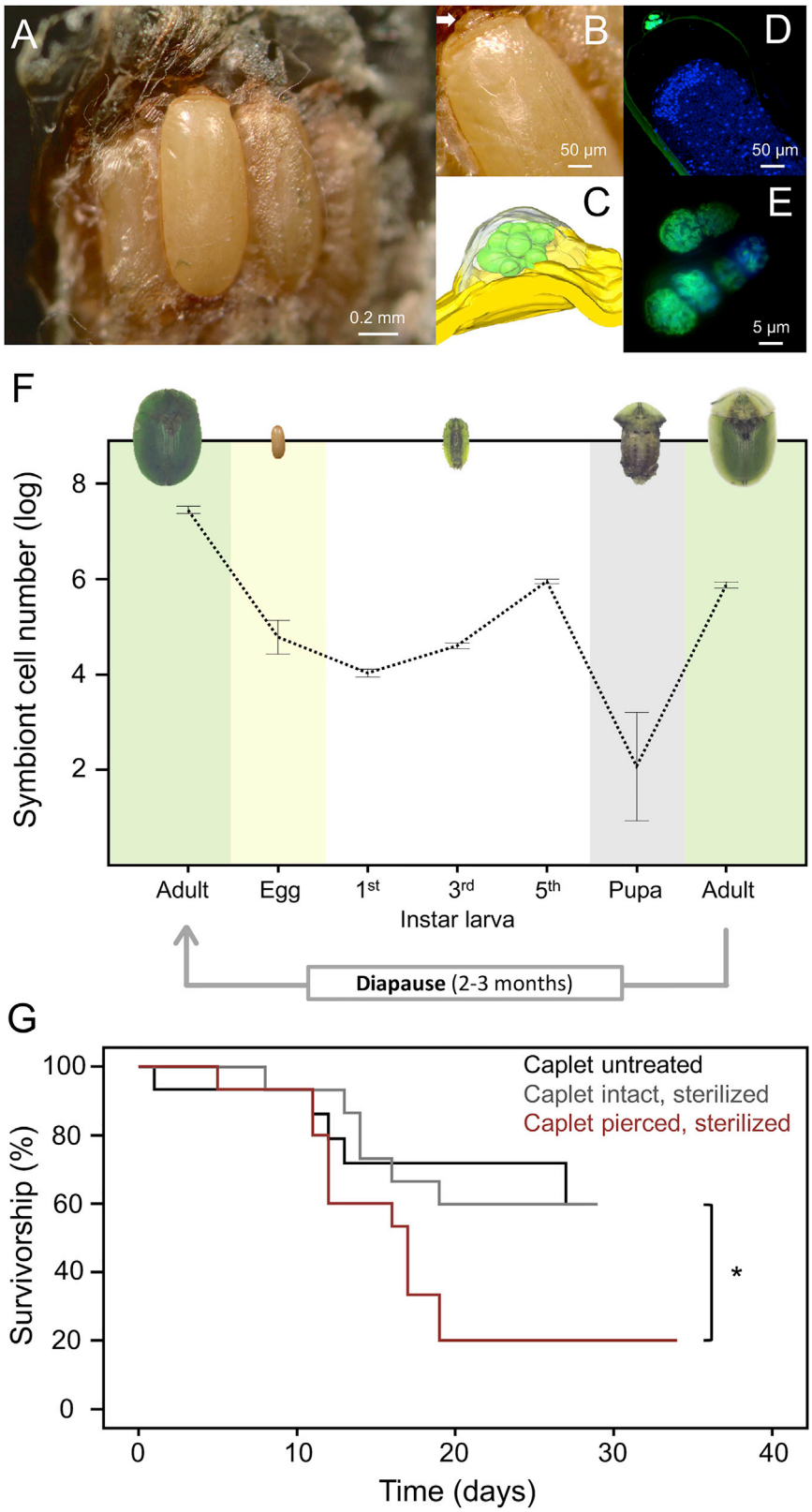

Figure 2. Transmission Route, In-Host Population Dynamics, and Symbiotic Impact of *Stammera*

(A and B) *Cassida rubiginosa* eggs (A) topped with (B) caplets (arrow) at the anterior pole.

(C) 3D-reconstruction of the egg caplet and the enclosed spheres.

(D and E) FISH of a cross-section featuring an egg (D) and its caplet (E) highlighting the localization of *Stammera* within the spheres.

(F) Symbiont population dynamics throughout host development following the quantification of 16S rRNA gene copy numbers. Whiskers denote the range.

(G) Survivorship rates (egg to adult eclosion) of *C. rubiginosa* following experimental sterilization of the egg caplet. Line coloration signifies the experimental treatment. The asterisk indicates significant differences between treatments ($p < 0.05$; Kaplan-Meier, Tarone-Ware test). Scale bars are included for reference.

See also Table S2.

rhamnogalacturonan I (Figure 3F). Additionally, we were able to annotate CorA, a magnesium/nickel/cobalt membrane transporter known to regulate pectinase production in γ-proteobacteria (Kersey et al., 2012) and SecA, a general translocation membrane protein with a demonstrated capacity for the extracellular export of pectinases in Gram-negative bacteria (He et al., 1991).

Host Pectinolytic Metabolism Outsourced to *Stammera*

Simultaneous host and symbiont transcriptomic analysis examining differential gene expression between the foregut symbiotic organ and the beetle's whole body (Bioproject: PRJNA414435) yielded insights into the indispensable role of *Stammera* towards mediating its host's ability to process and break down pectin. Sequence similarity and BLAST searches identified two putative pectin-degrading genes across the symbiotic organ and the whole body samples, both of which were exact matches to *Stammera*'s PG- and RL-coding sequences. Strikingly, no host-associated, or any other, transcripts coding for pectinases could be recovered, in contrast to previous findings of host-encoded PGs across a range of phytophagous beetles, specifically weevils, long-horn beetles, and leaf beetles (Table S4) (Pauchet et al., 2009, 2010, 2014; Kirsch et al., 2012, 2014, 2016; Keeling et al., 2013)—indicating that the symbiont likely represents the sole source of pectinolysis in *C. rubiginosa*. Unsurprisingly, given the specific localization of the symbionts, pectinase expression was found to be significantly enriched in the foregut symbiotic organs relative to the rest of the insect's body (Figure 3G; $p < 0.0001$; ANOVA), highlighting the importance of the symbiont-bearing structures to the host's pectinolytic metabolism.

Extending our search beyond pectinases revealed that *C. rubiginosa*'s own transcriptional profile includes the same endogenous plant cell wall degrading enzymes (PCWDEs) targeting cellulose and hemicellulose previously reported in other phytophagous beetles (Table S4), originating from ancient as well as recent, lineage-specific horizontal gene transfer events (Wybouw et al., 2016). This includes cellulolytic enzymes belonging to the glycoside hydrolase families 9, 45, as well as 48 (Table S4). Additionally, we identified contigs corresponding to several xylanases capable of metabolizing the hemicellulose xylan, consistent with previous findings in the coffee berry borer (Padilla-Hurtado et al., 2012). The presence of these cellulolytic enzymatic families verifies that (1) the lack of endogenous PGs is not an artifact of low transcriptome coverage, (2) cellulose and hemicellulose are degraded by endogenous enzymes in *C. rubiginosa* in a manner similar to other phytophagous beetles, (3) the outsourcing of pectinolytic metabolism to the symbiont did not extend to other enzymatic classes, and (4) the symbiont's PG and RL perfectly complement the endogenous plant cell wall degrading enzymatic pathways of the host.

Functional Characterization and Localization of Symbiont-Produced Polygalacturonase

To describe the functional properties of *Stammera*'s pectinolytic enzymes, we aimed for biochemical characterization following heterologous expression in *Escherichia coli*. However, this approach was only successful for the symbiont's PG and not the RL, despite the use of multiple different expression conditions, vectors, and various cell lines (for details see the STAR Methods). Agarose diffusion assays using Ruthenium red-stained plates containing polygalacturonic acid (demethylated homogalacturonan) revealed the PG to be functionally active, evidenced by the clear halo forming around the inoculation site relative to the negative control (Figure 4A). The analysis of breakdown products through a thin-layer-chromatogram (TLC) indicated that the PG is an endo-active enzyme capable of cleaving homogalacturonan into galacturonic acid oligomers, as well as trimers, dimers, and monomers (Figures 4B and S3). In quantifying the enzyme's hydrolytic activity across a variety of homogalacturonic substrates, the symbiont's PG demonstrated greatest efficiency in the presence of demethylated forms of pectin, specifically polygalacturonic acid (Figure 4C). The *Stammera*-produced PG was localized within *C. rubiginosa* using a specific antibody. Immunostaining cross sections revealed substantial PG buildup in the foregut symbiotic organs (Figure 4D), in line with a transcriptional profile indicative of an enriched pectinolytic metabolism in these structures (Figure 3G).

Aposymbiosis Results in a Diminished Pectinolytic Phenotype in *C. rubiginosa*

To functionally characterize the RL and to confirm the transcriptomic insights implicating *Stammera* as the sole source of pectinase activity within its leaf beetle host, we assessed the degree of hydrolysis of polygalacturonic acid and rhamnogalacturonan I using crude protein extracts collected from pooled whole-guts (foregut, symbiotic organs, midgut, and hindgut) emanating from symbiotic or aposymbiotic 3rd instar larvae. Agarose diffusion assays revealed symbiotic *C. rubiginosa* to harbor pectinolytic enzymes targeting both pectic substrates (Figure 5A)—in line with our annotation of a PG and RL in *Stammera*'s genome (Figure 3E). Conversely, protein extracts from aposymbiotic larvae produced drastically reduced halos following injection into agarose plates inundated with either of the two pectic substrates (Figure 5A). While a TLC of pectin's breakdown products highlighted the presence of galacturonic acid monomers in the guts of symbiotic larvae, only larger polysaccharidic subunits could be detected in the aposymbiotic individuals (Figures 5B and S4), indicative of a compromised pectinolytic metabolism following symbiont elimination. Considering that the leaf beetle's transcriptional profile revealed a dearth of pectin-degrading genes beyond those annotated in *Stammera*'s genome, we hypothesize that the residual pectinolytic activity observed in aposymbiotic insects (Figure 5A) is a product of plant-produced pectinases (Ogawa et al., 2009; Domingo et al., 1998) released into the gut lumen following mechanical processing of ingested foliage.

As expected, symbiont loss did not impact the cellulolytic capacity of *C. rubiginosa*, evidenced by the comparable halos observed on agar plates containing carboxymethylcellulose following incubation with symbiotic and aposymbiotic crude protein extracts collected from pooled whole-guts (Figure S5). This is consistent with the annotation of putative host-associated cellulases and hemicellulases in the *C. rubiginosa* transcriptome (Table S4).

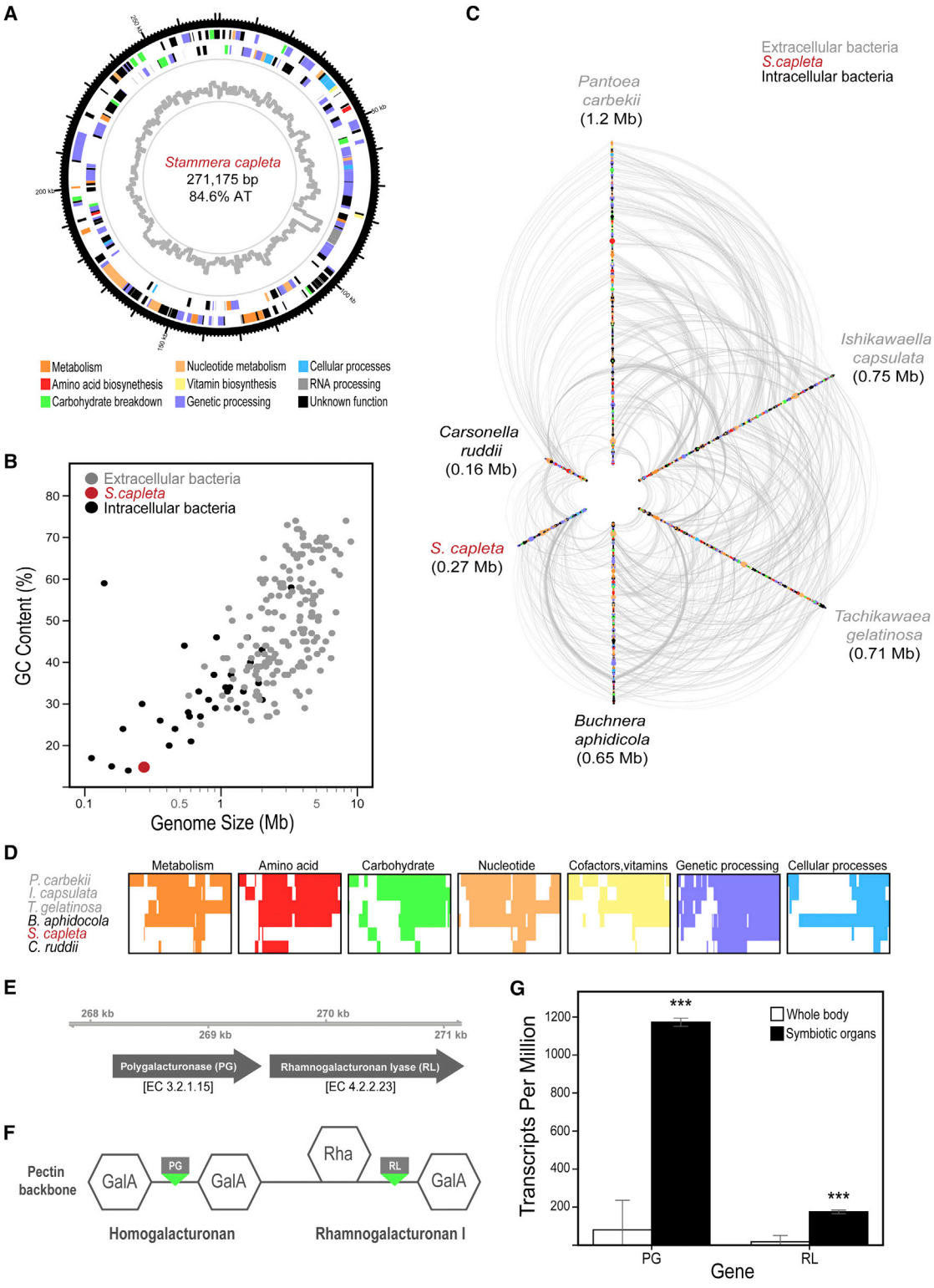

Figure 3. Drastically Reduced Extracellular Symbiont Genome Retains a Pectinolytic Metabolism

(A) Circular view of the *Stammera* genome. Internal CDS circles indicate annotated functional KEGG categories differentiated by coloration. Gray circle denotes relative GC content.

(B) Relationship between genome size and GC content for sequenced bacterial genomes. Colors denote intracellular (black), extracellular (gray) bacteria and *Stammera* (red, extracellular).

(legend continued on next page)

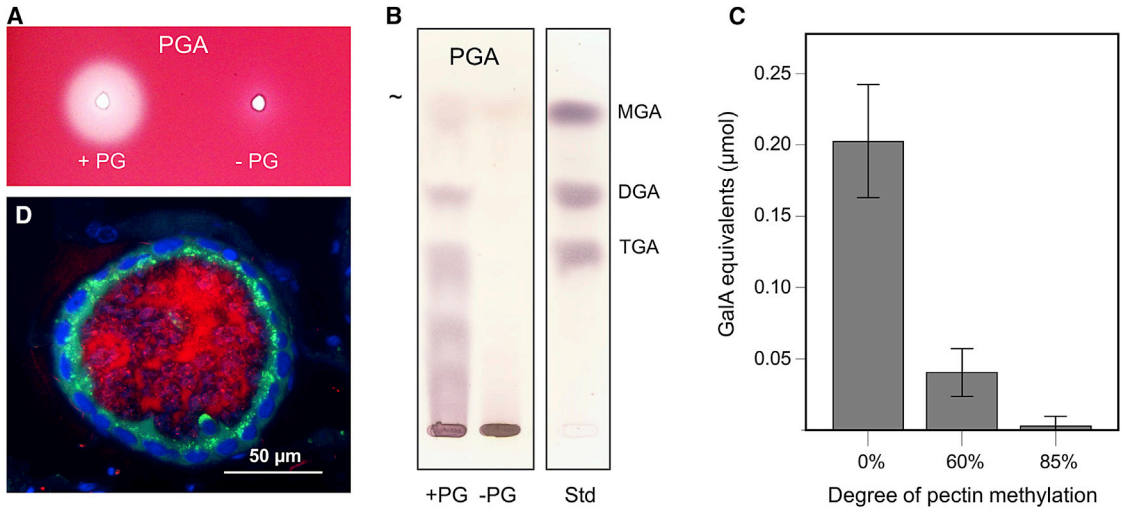

Figure 4. Functional Characterization and Localization of *Stammera*-Produced Polygalacturonase

(A) Agarose diffusion assay featuring crude protein extracts from *Escherichia coli* heterologously expressing the symbiont's polygalacturonase (+PG) and a negative control of non-transfected cells (−PG) following application to a gel containing polygalacturonic acid (PGA).

(B) Thin-layer chromatogram of +PG and −PG activity assays against PGA. Std, standard; MGA, mono-galacturonic acid; DGA, di-galacturonic acid; TGA, tri-galacturonic acid. Impurities are designated by ∼. Gaps denote an abridged version of the original gel (Figure S3).

(C) Quantification of PG activity relative to the degree of pectin methylation (0%–85%). Hydrolytic activity is expressed in galacturonic acid (GalA) equivalents (μmol) released. Whiskers denote the range.

(D) Cross section of a foregut symbiotic organ stained with a PG-targeting antibody (red). DAPI (blue) was used for counterstaining.

DISCUSSION

Some of the most elaborate and best documented symbioses across the Metazoa feature insects specializing on nutritionally imbalanced diets (Douglas, 2010; McFall-Ngai et al., 2013; Hansen and Moran, 2014). Given a mutual co-dependency, many symbionts evolve in parallel with their hosts, reflected in an intertwined co-evolutionary history that is stabilized through adaptations ensuring faithful trans-generational transfer and metabolic integration (Salem et al., 2015). Convergent patterns of reductive genome evolution commonly afflict endosymbionts in stable symbiotic continuums (Moran et al., 2008). Impacted by population bottlenecks and reduced recombination rates (Kuo et al., 2009), these genomes typically feature AT-biased nucleotide compositions and reduced sizes due to the deletion of non-essential genes (Moran et al., 2008). This paradigm allows us to explain the unprecedented genome minimization exhibited by *Stammera* as an extracellular microbe by taking into account: (1) its restricted localization in discrete symbiotic organs within *C. rubiginosa* (Figure 1) and during transmission (Figures 2A–2E), and (2) experiencing one of the sharpest symbiont population bottlenecks recorded to date, where a minuscule fraction (0.02%) of the parent population is available to newly emerging adults (Figure 2F). We do note that the symbiotic organs represent highly specialized structures that may offer many of the nutritional qualities of intracellular environments (e.g., bacteriocytes).

Beyond ensuring faithful transfer of an obligate symbiont to future host generations, the evolution of the egg caplet may have afforded greater metabolic stability to *Stammera* by drastically reducing its exposure to abiotic stresses during vertical transmission (Figures 2A–2E). Such a structure guarantees symbiont encapsulation throughout host development to a degree typically observed in partnerships where symbionts are transferred intracellularly during embryogenesis or oogenesis (Koga et al., 2012; Luan et al., 2016). A greater developmental coupling between *Stammera* and its host likely relaxed selection to maintain genes coding for basic cellular functions that are otherwise present in genomes belonging to extracellular bacteria, including some of the smallest; for example: the human pathogen *Mycoplasma genitalium* (0.58 Mb) (Fraser et al., 1995) or the stinkbug symbionts *Tachikawaea gelatinosa* (0.71 Mb) (Kaiwa et al., 2014) and *Ishikawalla capsulata* (0.75 Mb) (Nikoh et al., 2011). Notably absent metabolic pathways in *Stammera*'s genome include those coding for the Krebs cycle, phospholipid, and nucleotide biosynthesis, as well as other

(C and D) Hive plot (C) and heatmaps (D) (based on Table S3) comparing the functional gene repertoires of *Stammera* and representative intracellular and extracellular γ-proteobacterial insect symbionts. Node and box colors are based on KEGG's CDS.

(E and F) Annotated polygalacturonase (PG) and rhamnogalacturonan lyase (RL), alongside their Enzyme Commission (EC) numbers, in *Stammera*'s genome (E) targeting the homogalacturonan and rhamgalacturonan I pectic classes (F), respectively.

(G) Differential expression of PG and RL in the foregut symbiotic organs relative to the whole body. Asterisks indicate significant differences ($p < 0.0001$; ANOVA). Whiskers denote the range.

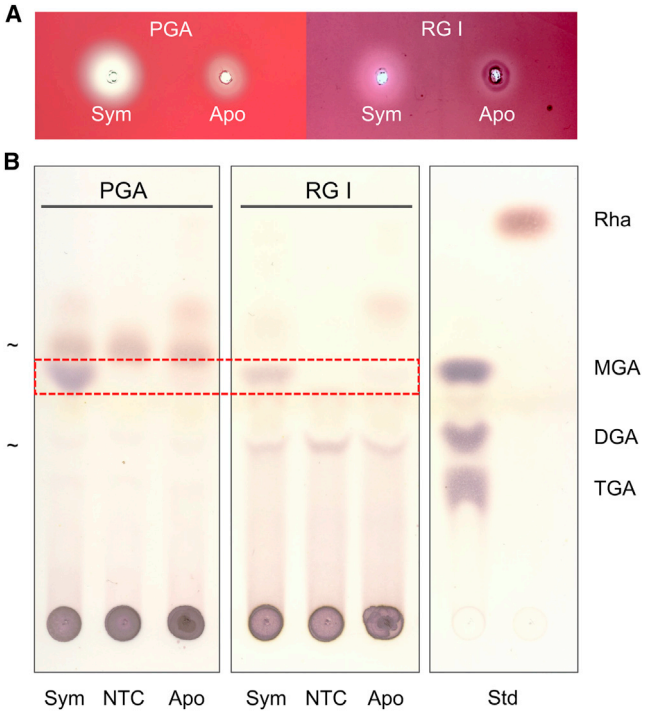

Figure 5. Symbiont Elimination Diminishes Pectinolytic Capacity in *Cassida rubiginosa*

(A) Agarose diffusion assays depicting pectinase activity in symbiotic (Sym) and aposymbiotic (Apo) larvae using gut protein extracts following application to gels containing polygalacturonic acid (PGA) and rhamnogalacturonan I (RG I).

(B) Thin layer chromatogram illustrating breakdown products of pectinase activity in Sym, Apo, and a no template control (NTC) assays against PGA and RG I. Std., standard; MGA, mono-galacturonic acid; DGA, di-galacturonic acid; TGA, tri-galacturonic acid; Rha, rhamnose. Impurities are designated by ~. Dashed box highlights MGA differences across treatments. Gaps denote an abridged version of the original gel (Figure S4).

primary processes that are essential for a microbe subsisting in a free-living state, however brief. While the chemical makeup of the egg caplet is unknown, we hypothesize it to be endowed with sufficient nutrients to sustain the survival and, possibly, growth of metabolically-deficient *Stammera* cells while the embryo develops within its chorion.

Characteristically enriched in most tiny endosymbiont genomes are gene categories coding for informational processes (translation, transcription, and replication) and the biosynthesis of essential nutrients underlying the symbioses (Moran et al., 2008). Reflecting their biological roles, essential amino acid and B vitamin pathways are functionally conserved across the genomes of primary endosymbionts of sap- and blood-feeding insects, respectively (Shigenobu et al., 2000; Akman et al., 2002). Consistent with these examples, *Stammera* with its streamlined metabolic profile complements an obligately folivorous host through the production of exoenzymes that are essential to the insect's digestive biology. Unlike other leaf beetles (Kirsch et al., 2012, 2014), *C. rubigionsa's* arsenal of endogenous PCWDEs does not include pectinases (Table S4) and the insect instead relies on symbiont-produced PGs and RLs to target the two most abundant polymers of the pectic matrix: homogalacturonan and rhamnogalacturonan I. In line with a clear beneficial impact (Figure 2G), a symbiont-conferred pectinolytic phenotype (Figure 5) may provide a selective advantage by allowing the insect to breach the plant cell wall barrier that impedes its access to the cytosol, thereby increasing the digestive efficacy of consumed foliage. This is consistent with our heterologous characterization of the symbiont's PG as an endo-active enzyme capable of hydrolyzing pectin at random intervals into galacturonic acid oligomers, as well as dimers and monomers (Figure 4B). While the predominance of galacturonic acid monomers as breakdown products in the guts of symbiont-harboring *C. rubiginosa* (Figure 5B) does not perfectly mirror the activity assays reported for the recombinant PG, the discrepant profiles can speculatively be ascribed to: (1) variation in protein folding patterns following export, with downstream impact on function, (2) differential incubation time and overall abundance of symbiont-produced PGs in the gut relative to protein extracts from *E. coli*, or (3) the unknown functional and likely synergistic features of *Stammera*-produced RLs following unsuccessful heterologous expression efforts.

As pectin degradation facilitates downstream breakdown of other primary cell wall components like cellulose and hemicellulose (De Lorenzo and Ferrari, 2002; Blackman et al., 2015), the location of the symbiotic organs near the foregut (Figures 1C and 1D) reinforces *Stammera*'s proposed biological role. Unlike nutrient-supplementing symbionts, *Stammera* upgrades its host's diet through the production of digestive enzymes that function in the extracellular matrix beyond the walls of the gut lumen, likely selecting against the symbiont transitioning to an intracellular lifestyle given the complications associated with bacterial enzyme translocation across eukaryotic host membranes. This is consistent with the extracellular localization of cellulolytic microbes in termites (Tokuda and Watanabe, 2007; Warnecke et al., 2007), cockroaches (Dietrich et al., 2014), and beetles (Vazquez-Arista et al., 1997), where cellulases require no further processing following export from symbiont cells (but see O'Connor et al., 2014). Thus, despite a high degree of metabolic and developmental integration with its host, the extracellularity of *Stammera* may in fact facilitate the delivery of PGs and RLs to their target substrates in the gut.

Beyond the intricacies of how an insect contends with the pectin it ingests, our findings highlight the convergent adaptations evolved by animals to exploit herbivorous diets. Specifically, horizontal gene transfer and symbiosis seem to confer the same adaptation across phytophagous beetles in a binary manner. The common ancestor to all weevils, long-horn and leaf beetles is estimated to have acquired a PG from an ascomycete fungus ~200 million years ago (Kirsch et al., 2014), coinciding with, and likely enabling, the transition to herbivory. While numerous rounds of gene duplication and subfunctionalization of PGs took place as phytophagous beetles diversified, there were also loss and replacement events (Kirsch et al., 2014). This dynamic pattern of PG gene transfer and loss may help explain the acquisition of *Stammera* and the subsequent outsourcing of a pectinolytic metabolism by

C. rubiginosa to its symbiont. Here, the symbiont's ability to produce pectinases targeting both homogalacturonan and rhamnogalacturonan I would have expanded the leaf beetle's digestive capacity, because the ancestral horizontal transfer event only involved PGs capable of cleaving the former of the two pectic substrates. Across the screened transcriptomes of leaf beetles (Table S4) (Pauchet et al., 2009, 2010, 2014; Kirsch et al., 2012, 2014, 2016), no RLs have thus far been annotated. While speculative, the acquisition of a symbiont capable of hydrolyzing pectin with greater efficiency—as a consequence of enzymatic synergy (Bonnin et al., 2002; Laatu and Condemine, 2003) or to counter plant enzyme inhibitors (Casasoli et al., 2009)—may have superseded selection for a leaf beetle to endogenously maintain PGs, potentially explaining the loss of horizontally acquired pectinases in *C. rubiginosa* in wake of its partnership with *Stammera*.

In characterizing the association between *Stammera* and tortoise leaf beetles, we describe a symbiosis defined by the microbe's ability to synthesize and export enzymes that upgrade the digestive capacity of its host. In doing so, we (1) demonstrate the multitude of strategies deployed by herbivorous insects as they contend with the complex plant polysaccharides that dominate their diet, (2) extend the range of known symbiotic factors enriched within tiny endosymbiont genomes beyond those involved in the supplementation of essential nutrients, and (3) highlight that extreme genomic degeneracy in bacteria is not an exclusive feature of intracellularity.

Description of "*Candidatus* Stammera capleta"

Commemorating original histological descriptions by Stammer (1936), we assign *Stammera* as the generic name, while *capleta* reflects the unique egg-associated structures utilized by the beetles to vertically transmit their symbionts. Uncultured, Gram-negative, non-motile, coccoid as well as rod-shaped bacteria of ~2–4 μm in diameter that can be assigned to the Enterobacteriaceae (γ-proteobacteria) on the basis of their 16S rRNA gene sequence. The bacteria live symbiotically within specialized organs associated with the foregut of larval and adult *C. rubiginosa*.

STAR★METHODS

Detailed methods are provided in the online version of this paper and include the following:

- KEY RESOURCES TABLE
- CONTACT FOR REAGENT AND RESOURCE SHARING
- EXPERIMENTAL MODEL AND SUBJECT DETAILS
- METHOD DETAILS
  - Bacterial tag-encoded FLX amplicon pyrosequencing (bTEFAP) and data analysis
  - Phylogenetic analysis
  - Diagnostic PCR screening
  - Symbiont localization by fluorescence *in situ* hybridization (FISH)
  - 3D-reconstruction of symbiont-bearing egg caplets
  - Quantitative PCR
  - Experimental manipulation of the symbiont-bearing egg caplet
  - Symbiont genome sequencing, assembly, and annotation
  - Transcriptome sequencing, assembly, and annotation and PCWDE identification
  - Heterologous pectinase expression and purification
  - Enzymatic assays
  - Immunohistochemistry
- QUANTIFICATION AND STATISTICAL ANALYSIS
- DATA AND SOFTWARE AVAILABILITY

SUPPLEMENTAL INFORMATION

Supplemental Information includes five figures, four tables, and one movie and can be found with this article online at https://doi.org/10.1016/j.cell.2017.10.029.

AUTHOR CONTRIBUTIONS

H.S., M.K., and A.B. conceived the study. H.S. and M.C. collected specimens and performed bioassays. H.S., A.B., and K.F. carried out the molecular work. E.B. and H.S. performed the genome sequencing, assembly, and analysis. E.B., R. Kirsch, H.S., and H.V. carried out transcriptome sequencing, assembly, and analysis. R. Kirsch performed the enzymatic assays. B.W. and H.S. conducted microscopy. R. Koga, K.F., and T.F. contributed immunohistochemical data. H.S. wrote the manuscript. All authors edited and commented on the paper.

ACKNOWLEDGMENTS

We thank Yannick Pauchet for insightful discussions on the experimental setup and Nicole Gerardo, Amanda Gibson, Wen-Hao Tan, and Jaap de Roode for helpful comments on an earlier draft of the manuscript. We thank Sarah Jackman for her assistance in beetle collection and maintenance. Financial support from the Max Planck Society, the Alexander von Humboldt Foundation, and the German Science Foundation (KI1917/1-1) is gratefully acknowledged.

Received: September 6, 2017
Revised: October 10, 2017
Accepted: October 17, 2017
Published: November 16, 2017

SUPPORTING CITATIONS

The following references appear in the Supplemental Information: Acuña et al. (2012), Aw et al. (2010), Doostdara et al. (1997), McKenna et al. (2016), Pauchet and Heckel (2013), Shen et al. (1996), Shen et al. (1999), Shen et al. (2003), and Shen et al. (2005).

REFERENCES

Abbott, D.W., and Boraston, A.B. (2008). Structural biology of pectin degradation by Enterobacteriaceae. Microbiol. Mol. Biol. Rev. *72*, 301–316.

Acuña, R., Padilla, B.E., Flórez-Ramos, C.P., Rubio, J.D., Herrera, J.C., Benavides, P., Lee, S.J., Yeats, T.H., Egan, A.N., Doyle, J.J., and Rose, J.K. (2012). Adaptive horizontal transfer of a bacterial gene to an invasive insect pest of coffee. Proc. Natl. Acad. Sci. USA *109*, 4197–4202.

Akman, L., Yamashita, A., Watanabe, H., Oshima, K., Shiba, T., Hattori, M., and Aksoy, S. (2002). Genome sequence of the endocellular obligate symbiont of tsetse flies, *Wigglesworthia glossinidia*. Nat. Genet. *32*, 402–407.

Alfano, J.R., and Collmer, A. (1996). Bacterial pathogens in plants: life up against the wall. Plant Cell *8*, 1683–1698.

Aw, T., Schlauch, K., Keeling, C.I., Young, S., Bearfield, J.C., Blomquist, G.J., and Tittiger, C. (2010). Functional genomics of mountain pine beetle (Dendroctonus ponderosae) midguts and fat bodies. BMC Genomics *11*, 215.

Aziz, R.K., Bartels, D., Best, A.A., DeJongh, M., Disz, T., Edwards, R.A., Formsma, K., Gerdes, S., Glass, E.M., Kubal, M., et al. (2008). The RAST Server: rapid annotations using subsystems technology. BMC Genomics *9*, 75.

Bankevich, A., Nurk, S., Antipov, D., Gurevich, A.A., Dvorkin, M., Kulikov, A.S., Lesin, V.M., Nikolenko, S.I., Pham, S., Prjibelski, A.D., et al. (2012). SPAdes: a new genome assembly algorithm and its applications to single-cell sequencing. J. Comput. Biol. *19*, 455–477.

Berasategui, A., Axelsson, K., Nordlander, G., Schmidt, A., Borg-Karlson, A.K., Gershenzon, J., Terenius, O., and Kaltenpoth, M. (2016). The gut microbiota of the pine weevil is similar across Europe and resembles that of other conifer-feeding beetles. Mol. Ecol. *25*, 4014–4031.

Blackman, L.M., Cullerne, D.P., Torreña, P., Taylor, J., and Hardham, A.R. (2015). RNA-Seq analysis of the expression of genes encoding cell wall degrading enzymes during infection of lupin (*Lupinus angustifolius*) by *Phytophthora parasitica*. PLoS ONE *10*, e0136899.

Boetzer, M., and Pirovano, W. (2012). Toward almost closed genomes with GapFiller. Genome Biol. *13*, R56.

Bolger, A.M., Lohse, M., and Usadel, B. (2014). Trimmomatic: a flexible trimmer for Illumina sequence data. Bioinformatics *30*, 2114–2120.

Bonnin, E., Dolo, E., Le Goff, A., and Thibault, J.F. (2002). Characterisation of pectin subunits released by an optimised combination of enzymes. Carbohydr. Res. *337*, 1687–1696.

Boto, L. (2014). Horizontal gene transfer in the acquisition of novel traits by metazoans. Proc. Biol. Sci. *281*, 20132450.

Burton, R.A., Gidley, M.J., and Fincher, G.B. (2010). Heterogeneity in the chemistry, structure and function of plant cell walls. Nat. Chem. Biol. *6*, 724–732.

Calderón-Cortés, N., Quesada, M., Watanabe, H., Cano-Camacho, H., and Oyama, K. (2012). Endogenous plant cell wall digestion: a key mechanism in insect evolution. Annu. Rev. Ecol. Evol. Syst. *43*, 45–71.

Caporaso, J.G., Kuczynski, J., Stombaugh, J., Bittinger, K., Bushman, F.D., Costello, E.K., Fierer, N., Peña, A.G., Goodrich, J.K., Gordon, J.I., et al. (2010). QIIME allows analysis of high-throughput community sequencing data. Nat. Methods *7*, 335–336.

Casasoli, M., Federici, L., Spinelli, F., Di Matteo, A., Vella, N., Scaloni, F., Fernandez-Recio, J., Cervone, F., and De Lorenzo, G. (2009). Integration of evolutionary and desolvation energy analysis identifies functional sites in a plant immunity protein. Proc. Natl. Acad. Sci. USA *106*, 7666–7671.

Danchin, E.G., Rosso, M.N., Vieira, P., de Almeida-Engler, J., Coutinho, P.M., Henrissat, B., and Abad, P. (2010). Multiple lateral gene transfers and duplications have promoted plant parasitism ability in nematodes. Proc. Natl. Acad. Sci. USA *107*, 17651–17656.

De Lorenzo, G., and Ferrari, S. (2002). Polygalacturonase-inhibiting proteins in defense against phytopathogenic fungi. Curr. Opin. Plant Biol. *5*, 295–299.

Dietrich, C., Köhler, T., and Brune, A. (2014). The cockroach origin of the termite gut microbiota: patterns in bacterial community structure reflect major evolutionary events. Appl. Environ. Microbiol. *80*, 2261–2269.

Domingo, C., Roberts, K., Stacey, N.J., Connerton, I., Ruíz-Teran, F., and McCann, M.C. (1998). A pectate lyase from *Zinnia elegans* is auxin inducible. Plant J. *13*, 17–28.

Doostdara, H., McCollum, T.G., and Mayera, R.T. (1997). Purification and characterization of an endo-polygalacturonase from the gut of West Indies sugarcane rootstalk borer weevil (Diaprepes abbreviatus L.) larvae. Comp. Biochem. Physiol. B *118*, 861–867.

Douglas, A.E. (2010). The Symbiotic Habit (Princeton University Press).

Engel, P., Martinson, V.G., and Moran, N.A. (2012). Functional diversity within the simple gut microbiota of the honey bee. Proc. Natl. Acad. Sci. USA *109*, 11002–11007.

Fraser, C.M., Gocayne, J.D., White, O., Adams, M.D., Clayton, R.A., Fleischmann, R.D., Bult, C.J., Kerlavage, A.R., Sutton, G., Kelley, J.M., et al. (1995). The minimal gene complement of *Mycoplasma genitalium*. Science *270*, 397–403.

Gilbert, H.J. (2010). The biochemistry and structural biology of plant cell wall deconstruction. Plant Physiol. *153*, 444–455.

Götz, S., García-Gómez, J.M., Terol, J., Williams, T.D., Nagaraj, S.H., Nueda, M.J., Robles, M., Talón, M., Dopazo, J., and Conesa, A. (2008). High-throughput functional annotation and data mining with the Blast2GO suite. Nucleic Acids Res. *36*, 3420–3435.

Gouy, M., Guindon, S., and Gascuel, O. (2010). SeaView version 4: A multiplatform graphical user interface for sequence alignment and phylogenetic tree building. Mol. Biol. Evol. *27*, 221–224.

Hansen, A.K., and Moran, N.A. (2014). The impact of microbial symbionts on host plant utilization by herbivorous insects. Mol. Ecol. *23*, 1473–1496.

He, S.Y., Schoedel, C., Chatterjee, A.K., and Collmer, A. (1991). Extracellular secretion of pectate lyase by the *Erwinia chrysanthemi* out pathway is dependent upon Sec-mediated export across the inner membrane. J. Bacteriol. *173*, 4310–4317.

Hosokawa, T., Kikuchi, Y., and Fukatsu, T. (2007). How many symbionts are provided by mothers, acquired by offspring, and needed for successful vertical transmission in an obligate insect-bacterium mutualism? Mol. Ecol. *16*, 5316–5325.

Jacobs, C.G., Steiger, S., Heckel, D.G., Wielsch, N., Vilcinskas, A., and Vogel, H. (2016). Sex, offspring and carcass determine antimicrobial peptide expression in the burying beetle. Sci. Rep. *6*, 25409.

Jayani, R.S., Saxena, S., and Gupta, R. (2005). Microbial pectinolytic enzymes: a review. Process Biochem. *40*, 2931–2944.

Kaiwa, N., Hosokawa, T., Nikoh, N., Tanahashi, M., Moriyama, M., Meng, X.Y., Maeda, T., Yamaguchi, K., Shigenobu, S., Ito, M., and Fukatsu, T. (2014). Symbiont-supplemented maternal investment underpinning host's ecological adaptation. Curr. Biol. *24*, 2465–2470.

Keeling, C.I., Yuen, M.M., Liao, N.Y., Docking, T.R., Chan, S.K., Taylor, G.A., Palmquist, D.L., Jackman, S.D., Nguyen, A., Li, M., et al. (2013). Draft genome of the mountain pine beetle, *Dendroctonus ponderosae Hopkins,* a major forest pest. Genome Biol. *14*, R27.

Kersey, C.M., Agyemang, P.A., and Dumenyo, C.K. (2012). CorA, the magnesium/nickel/cobalt transporter, affects virulence and extracellular enzyme production in the soft rot pathogen *Pectobacterium carotovorum*. Mol. Plant Pathol. *13*, 58–71.

Kirsch, R., Wielsch, N., Vogel, H., Svatoš, A., Heckel, D.G., and Pauchet, Y. (2012). Combining proteomics and transcriptome sequencing to identify active plant-cell-wall-degrading enzymes in a leaf beetle. BMC Genomics *13*, 587.

Kirsch, R., Gramzow, L., Theißen, G., Siegfried, B.D., Ffrench-Constant, R.H., Heckel, D.G., and Pauchet, Y. (2014). Horizontal gene transfer and functional diversification of plant cell wall degrading polygalacturonases: Key events in the evolution of herbivory in beetles. Insect Biochem. Mol. Biol. *52*, 33–50.

Kirsch, R., Heckel, D.G., and Pauchet, Y. (2016). How the rice weevil breaks down the pectin network: Enzymatic synergism and sub-functionalization. Insect Biochem. Mol. Biol. *71*, 72–82.

Koga, R., Meng, X.Y., Tsuchida, T., and Fukatsu, T. (2012). Cellular mechanism for selective vertical transmission of an obligate insect symbiont at the bacteriocyte-embryo interface. Proc. Natl. Acad. Sci. USA *109*, E1230–E1237.

Komaki, K., and Ishikawa, H. (1999). Intracellular bacterial symbionts of aphids possess many genomic copies per bacterium. J. Mol. Evol. *48*, 717–722.

Komaki, K., and Ishikawa, H. (2000). Genomic copy number of intracellular bacterial symbionts of aphids varies in response to developmental stage and morph of their host. Insect Biochem. Mol. Biol. *30*, 253–258.

Kumar, S., Stecher, G., and Tamura, K. (2016). MEGA7: Molecular Evolutionary Genetics Analysis version 7.0 for bigger datasets. Mol. Biol. Evol. *33*, 1870–1874.

Kuo, C.H., Moran, N.A., and Ochman, H. (2009). The consequences of genetic drift for bacterial genome complexity. Genome Res. *19*, 1450–1454.

Laatu, M., and Condemine, G. (2003). Rhamnogalacturonate lyase RhiE is secreted by the out system in *Erwinia chrysanthemi*. J. Bacteriol. *185*, 1642–1649.

Langmead, B., and Salzberg, S.L. (2012). Fast gapped-read alignment with Bowtie 2. Nat. Methods *9*, 357–359.

Luan, J.B., Shan, H.W., Isermann, P., Huang, J.H., Lammerding, J., Liu, S.S., and Douglas, A.E. (2016). Cellular and molecular remodelling of a host cell for vertical transmission of bacterial symbionts. Proc. Biol. Sci. *283*, 20160580.

Martens, E.C., Lowe, E.C., Chiang, H., Pudlo, N.A., Wu, M., McNulty, N.P., Abbott, D.W., Henrissat, B., Gilbert, H.J., Bolam, D.N., and Gordon, J.I. (2011). Recognition and degradation of plant cell wall polysaccharides by two human gut symbionts. PLoS Biol. *9*, e1001221.

McCutcheon, J.P., McDonald, B.R., and Moran, N.A. (2009). Origin of an alternative genetic code in the extremely small and GC-rich genome of a bacterial symbiont. PLoS Genet. *5*, e1000565.

McFall-Ngai, M., Hadfield, M.G., Bosch, T.C., Carey, H.V., Domazet-Lošo, T., Douglas, A.E., Dubilier, N., Eberl, G., Fukami, T., Gilbert, S.F., et al. (2013). Animals in a bacterial world, a new imperative for the life sciences. Proc. Natl. Acad. Sci. USA *110*, 3229–3236.

McKenna, D.D., Scully, E.D., Pauchet, Y., Hoover, K., Kirsch, R., Geib, S.M., Mitchell, R.F., Waterhouse, R.M., Ahn, S.J., Arsala, D., et al. (2016). Genome of the Asian longhorned beetle (Anoplophora glabripennis), a globally significant invasive species, reveals key functional and evolutionary innovations at the beetle-plant interface. Genome Biol. *17*, 227.

Miller, G.L. (1959). Use of Dinitrosalicylic acid reagent for determination of reducing sugars. Anal. Chem. *31*, 426–428.

Mohnen, D. (2008). Pectin structure and biosynthesis. Curr. Opin. Plant Biol. *11*, 266–277.

Moran, N.A. (2007). Symbiosis as an adaptive process and source of phenotypic complexity. Proc. Natl. Acad. Sci. USA *104* (*Suppl 1*), 8627–8633.

Moran, N.A., McCutcheon, J.P., and Nakabachi, A. (2008). Genomics and evolution of heritable bacterial symbionts. Annu. Rev. Genet. *42*, 165–190.

Nikoh, N., Hosokawa, T., Oshima, K., Hattori, M., and Fukatsu, T. (2011). Reductive evolution of bacterial genome in insect gut environment. Genome Biol. Evol. *3*, 702–714.

O'Connor, R.M., Fung, J.M., Sharp, K.H., Benner, J.S., McClung, C., Cushing, S., Lamkin, E.R., Fomenkov, A.I., Henrissat, B., Londer, Y.Y., et al. (2014). Gill bacteria enable a novel digestive strategy in a wood-feeding mollusk. Proc. Natl. Acad. Sci. USA *111*, E5096–E5104.

Ogawa, M., Kay, P., Wilson, S., and Swain, S.M. (2009). *ARABIDOPSIS* DEHISCENCE ZONE POLYGALACTURONASE1 (ADPG1), ADPG2, and QUARTET2 are Polygalacturonases required for cell separation during reproductive development in *Arabidopsis*. Plant Cell *21*, 216–233.

Padilla-Hurtado, B., Flórez-Ramos, C., Aguilera-Gálvez, C., Medina-Olaya, J., Ramírez-Sanjuan, A., Rubio-Gómez, J., and Acuña-Zornosa, R. (2012). Cloning and expression of an endo-1,4-β-xylanase from the coffee berry borer, *Hypothenemus hampei*. BMC Res. Notes *5*, 23.

Patel, D.D., Patel, A.K., Parmar, N.R., Shah, T.M., Patel, J.B., Pandya, P.R., and Joshi, C.G. (2014). Microbial and Carbohydrate Active Enzyme profile of buffalo rumen metagenome and their alteration in response to variation in the diet. Gene *545*, 88–94.

Pauchet, Y., Wilkinson, P., van Munster, M., Augustin, S., Pauron, D., and ffrench-Constant, R.H. (2009). Pyrosequencing of the midgut transcriptome of the poplar leaf beetle *Chrysomela tremulae* reveals new gene families in Coleoptera. Insect Biochem. Mol. Biol. *39*, 403–413.

Pauchet, Y., Wilkinson, P., Chauhan, R., and Ffrench-Constant, R.H. (2010). Diversity of beetle genes encoding novel plant cell wall degrading enzymes. PLoS ONE *5*, e15635.

Pauchet, Y., and Heckel, D.G. (2013). The genome of the mustard leaf beetle encodes two active xylanases originally acquired from bacteria through horizontal gene transfer. Proc. Biol. Sci. *280*, 20131021.

Pauchet, Y., Kirsch, R., Giraud, S., Vogel, H., and Heckel, D.G. (2014). Identification and characterization of plant cell wall degrading enzymes from three glycoside hydrolase families in the cerambycid beetle *Apriona japonica*. Insect Biochem. Mol. Biol. *49*, 1–13.

Pope, P.B., Mackenzie, A.K., Gregor, I., Smith, W., Sundset, M.A., McHardy, A.C., Morrison, M., and Eijsink, V.G. (2012). Metagenomics of the Svalbard reindeer rumen microbiome reveals abundance of polysaccharide utilization loci. PLoS ONE *7*, e38571.

Rose, J.K. (2003). The Plant Cell Wall (CRC Press).

Rye, C.S., and Withers, S.G. (2000). Glycosidase mechanisms. Curr. Opin. Chem. Biol. *4*, 573–580.

Salem, H., Florez, L., Gerardo, N., and Kaltenpoth, M. (2015). An out-of-body experience: the extracellular dimension for the transmission of mutualistic bacteria in insects. Proc. Biol. Sci. *282*, 20142957.

Sengupta, S., Yang, X., and Higgs, P.G. (2007). The mechanisms of codon reassignments in mitochondrial genetic codes. J. Mol. Evol. *64*, 662–688.

Shelomi, M., Danchin, E.G., Heckel, D., Wipfler, B., Bradler, S., Zhou, X., and Pauchet, Y. (2016). Horizontal gene transfer of pectinases from bacteria preceded the diversification of stick and leaf insects. Sci. Rep. *6*, 26388.

Shen, Z., Reese, J.C., and Reeck, G.R. (1996). Purification and characterization of polygalacturonase from the rice weevil, *Sitophilus oryzae* (Coleoptera: Curculionidae). Insect Biochem. Mol. Biol. *26*, 427–433.

Shen, Z., Manning, G., Reese, J.C., and Reeck, G.R. (1999). Pectin methylesterase from the rice weevil, *Sitophilus oryzae* (L.)(Coleoptera: Curculionidae): Purification and characterization. Insect Biochem. Mol. Biol. *29*, 209–214.

Shen, Z., Denton, M., Mutti, N., Pappan, K., Kanost, M.R., Reese, J.C., and Reeck, G.R. (2003). Polygalacturonase from Sitophilus oryzae: possible horizontal transfer of a pectinase gene from fungi to weevils. J. Insect Sci. *3*, 24.

Shen, Z., Pappan, K., Mutti, N.S., He, Q.J., Denton, M., Zhang, Y., Kanost, M.R., Reese, J.C., and Reeck, G.R. (2005). Pectinmethylesterase from the rice weevil, *Sitophilus oryzae*: cDNA isolation and sequencing, genetic origin, and expression of the recombinant enzyme. J. Insect Sci. *5*, 21.

Shigenobu, S., Watanabe, H., Hattori, M., Sakaki, Y., and Ishikawa, H. (2000). Genome sequence of the endocellular bacterial symbiont of aphids *Buchnera* sp. APS. Nature *407*, 81–86.

Sprockett, D.D., Piontkivska, H., and Blackwood, C.B. (2011). Evolutionary analysis of glycosyl hydrolase family 28 (GH28) suggests lineage-specific expansions in necrotrophic fungal pathogens. Gene *479*, 29–36.

Stammer, H.J. (1936). Studien an Symbiosen zwischen Käfern und Mikroorganismen. II. Die Symbiose des *Bromius obscurus* L. und der *Cassida*-Arten (Coleopt. Chrysomel.). Z. Morphol. Ökol. Tiere *30*, 682–697.

Sun, Y., Wolcott, R.D., and Dowd, S.E. (2011). Tag-encoded FLX amplicon pyrosequencing for the elucidation of microbial and functional gene diversity in any environment. Methods Mol. Biol. *733*, 129–141.

Tokuda, G., and Watanabe, H. (2007). Hidden cellulases in termites: revision of an old hypothesis. Biol. Lett. *3*, 336–339.

Underwood, W. (2012). The plant cell wall: a dynamic barrier against pathogen invasion. Front. Plant Sci. *3*, 85.

Van Borm, S., Wenseleers, T., Billen, J., and Boomsma, J.J. (2001). *Wolbachia* in leafcutter ants: a widespread symbiont that may induce male killing or incompatible matings. J. Evol. Biol. *14*, 805–814.

Vazquez-Arista, M., Smith, R.H., Olalde-Portugal, V., Hinojosa, R.E., Hernandez-Delgadillo, R., and Blanco-Labra, A. (1997). Cellulolytic bacteria in the

digestive system of *Prostephanus truncatus* (Coleoptera: Bostrichidae). J. Econ. Entomol. *90*, 1371–1376.

Vogel, H., Badapanda, C., Knorr, E., and Vilcinskas, A. (2014). RNA-sequencing analysis reveals abundant developmental stage-specific and immunity-related genes in the pollen beetle *Meligethes aeneus*. Insect Mol. Biol. *23*, 98–112.

Voragen, A.G., Coenen, G.J., Verhoef, R.P., and Schols, H.A. (2009). Pectin, a versatile polysaccharide present in plant cell walls. Struct. Chem. *20*, 263–275.

Warnecke, F., Luginbühl, P., Ivanova, N., Ghassemian, M., Richardson, T.H., Stege, J.T., Cayouette, M., McHardy, A.C., Djordjevic, G., Aboushadi, N., et al. (2007). Metagenomic and functional analysis of hindgut microbiota of a wood-feeding higher termite. Nature *450*, 560–565.

Weiss, B., and Kaltenpoth, M. (2016). Bacteriome-localized intracellular symbionts in pollen-feeding beetles of the genus *Dasytes* (Coleoptera, Dasytidae). Front. Microbiol. *7*, 1486.

Wybouw, N., Pauchet, Y., Heckel, D.G., and Van Leeuwen, T. (2016). Horizontal gene transfer contributes to the evolution of arthropod herbivory. Genome Biol. Evol. *8*, 1785–1801.

Yamao, F., Muto, A., Kawauchi, Y., Iwami, M., Iwagami, S., Azumi, Y., and Osawa, S. (1985). UGA is read as tryptophan in *Mycoplasma capricolum*. Proc. Natl. Acad. Sci. USA *82*, 2306–2309.

STAR★METHODS

KEY RESOURCES TABLE

REAGENT or RESOURCE	SOURCE	IDENTIFIER
Antibodies		
Anti-His(C-term)-HRP Antibody	Thermo Scientific	Cat# R931-25
Rabbit polyclonal anti-PG antibody	This paper	N/A
Anti-rabbit IgG goat antibody conjugated with peroxidase	Sigma-Aldrich	Cat#A9169
Anti-V5-HRP Antibody	Thermo Scientific	Cat# R96125
Bacterial and Virus Strains		
Candidatus Stammera capleta	This study	N/A
BL21 Star (DE3)	Thermo Scientific	Cat#C601003
BL21 Star (DE3)pLys	Thermo Scientific	Cat# C602003
NiCo21 (DE3)	New England Biolabs	Cat# C2529H
RV308	Dr. C. Haupt, Ulm, Germany	N/A
Biological Samples		
Cassida rubiginosa collected in Jena, Germany	This paper	N/A
Cassida rubiginosa collected in Tokyo, Japan	This paper	N/A
Cassida rubiginosa collected in Lincoln, NZ	This paper	N/A
Cassida rubiginosa collected in Missoula, USA	This paper	N/A
Chemicals, Peptides, and Recombinant Proteins		
Technovit8100	Kulzer	Cat#64709012
DAPI	Roth	Cat#6843.1 CAS-Nr.: 28718-90-3
QIAGEN DNeasy Blood & Tissue Kit	QIAGEN	Cat# 69506
Taq DNA polymerase	VWR	Cat# 89167-762
Triton X-100	Sigma	Cat# T8787-50ML
VectaShield	Vector Laboratories	Cat# H-1200
Bouin solution	Sigma	Cat# HT10132-1L
Epoxy Embedding Medium kit	Sigma	Cat# 45359-1EA-F
Entellan	Merck	Cat# 1079610100
SYBR Green Mix	QIAGEN	Cat# 204074
QIAGEN RNA Extraction kit	QIAGEN	Cat# 74104
BugBuster® 10X Protein Extraction Reagent - Novagen	Merck	Cat# 70921-4
Lysonase Bioprocessing Reagent	Merck	Cat# 71230-3
HisPur Cobalt Resin	Thermo Scientific	Cat# 89964
cOmplete, EDTA-free Protease Inhibitor Cocktail	Merck	Cat# 11873580001
Zeba Spin Desalting Columns, 7K MWCO, 5 mL	Thermo Scientific	Cat# 89892
Ruthenium Red	Sigma-Aldrich	Cat# R2751
Congo Red	Sigma-Aldrich	Cat# C6767
Orcinol monohydrate	Sigma-Aldrich	Cat# O1875
3,5-Dinitrosalicylic acid	Sigma-Aldrich	Cat# 128848
Pectin from citrus peel	Sigma-Aldrich	Cat# P9135
Pectin, esterified from citrus fruit	Sigma-Aldrich	Cat# P9561
Polygalacturonic Acid	Megazyme	Cat# P-PGACT
Rhamnogalacturonan I (Potato)	Megazyme	Cat# P-RHAM1
D-(+)-Galacturonic acid monohydrate	Santa Cruz Biotechnology	Cat# sc-257277

(*Continued on next page*)

Continued

REAGENT or RESOURCE	SOURCE	IDENTIFIER
Digalacturonic acid	Santa Cruz Biotechnology	Cat# sc-214891
Trigalacturonic acid	Santa Cruz Biotechnology	Cat# sc-222371
Critical Commercial Assays		
Overnight Express Autoinduction System 1 - Novagen	Merck	Cat# 71300-4
SuperSignal West HisProbe Kit	Thermo Scientific	Cat# 15168
Champion pET101 Directional TOPO Expression Kit	Thermo Scientific	Cat# K10101
Synthetic peptide Cys+YLTKTGSMNENSTG-OH	This study	N/A
Sf-900 II SFM	Thermo Scientific	Cat#10902088
FuGENE® HD Transfection Reagent	Promega	Cat# E2311
Critical Commercial Assays		
TSA-Plus Cyanine 3/Cyanine 5 System	PerkinElmer	Cat# NEL752001KT
Deposited Data		
Raw 16S rRNA profilling	This paper	NCBI: SRP119423
Transcriptome sequencing Bioproject ID	This paper	NCBI:PRJNA414435
Genome sequencing Bioproject ID	This paper	NCBI:PRJNA413589
Stammera genome identifier	This paper	NCBI: CP024013
Experimental Models: Organisms/Strains		
Cassida rubiginosa collected in Lincoln, NZ	This paper	N/A
Oligonucleotides		
FISH Probe: Cy5-Stammera F: TCATGTTGCCG TTCAACT	This paper	N/A
Primer: Stammera_F Forward: CAAGTTGAACG GCAACATGA	This paper	N/A
Primer: Stammera_R2 Reverse: GTACAAGGCCC GAGAACGTA	This paper	N/A
Primer: 16SWOLBF1 Forward: GGGATTRGCTT AGCCTCGCGAC	Van Borm et al., 2001	N/A
Primer: 16WOLBRA1 Reverse: TCATGTTGC CGTTCAACT	Van Borm et al., 2001	N/A
Primer: pET101-PG Forward: CACCATGGACA CCCGTAACGTGAAAGAACC	This paper	N/A
Primer: pET101-PG Reverse: TTGATAATTCGG GCAGATATTGCC	This paper	N/A
Primer: pMIB-PG Forward: TAATAAGCTTGGA CACCCGTAACGTGAAAGAACC	This paper	N/A
Primer: pMIB-PG Reverse: TAATCTCGAGTTG ATAATTCGGGCAGATATTGCC	This paper	N/A
Recombinant DNA		
Plasmid: pET-22b(+)-PG	Genscript	N/A
Plasmid: pET-22b(+)-RL	Genscript	N/A
Plasmid: pMIB/V5-His	Thermo Scientific	Cat# V803001
Software and Algorithms		
Zen 2	Carl Zeiss Microscopy GmbH	2.0.14283.302
Amira 6.3.0	FEI	9.18.13.3182
SeaView	Gouy et al., 2010	http://doua.prabi.fr/software/seaview
QIIME	Caporaso et al., 2010	http://qiime.org
Trimmomatic	Bolger et al., 2014	https://github.com/timflutre/trimmomatic
MEGA 7	Kumar et al., 2016	http://www.megasoftware.net

(*Continued on next page*)

Continued

REAGENT or RESOURCE	SOURCE	IDENTIFIER
Bowtie2	Langmead and Salzberg, 2012	http://bowtie-bio.sourceforge.net/bowtie2/index.shtml
Spades	Bankevich et al., 2012	http://bioinf.spbau.ru/spades
GapFiller	Boetzer and Pirovano, 2012	https://www.baseclear.com/genomics/bioinformatics/basetools/gapfiller
RAST	Aziz et al., 2008	http://rast.nmpdr.org
CLC Genomics Workbench v10.0.1	QIAGEN Bioinformatics	https://www.qiagenbioinformatics.com/products/clc-genomics-workbench/
Blast2GO PRO	Blast2GO	v4.1.5
SPSS	IBM	V17.0

CONTACT FOR REAGENT AND RESOURCE SHARING

Further information and requests for resources and reagents should be directed to and will be fulfilled by the Lead Contact, Hassan Salem (hssalem@emory.edu).

EXPERIMENTAL MODEL AND SUBJECT DETAILS

Thirteen *Cassida rubiginosa* (Coleoptera: Chrysomelidae) mating pairs were collected from the leaves of *Cirsium arvense* in Lincoln, New Zealand. The insects were reared in plastic containers in the lab. Eggs were collected from separate mating pairs ahead of experimental manipulation. The ootheca were used to generate representatives across the three treatments. Experimental larvae were reared at room temperature in separate Petri dishes and were provisioned daily with fresh *C. arvense* leaves. We cannot report on the sex ratios of the experimental insects due to the identical morphology shared across male and female larvae. Beetles were maintained and cared for in the laboratory according to the Institutional Animal Use and Care Guidelines.

METHOD DETAILS

Bacterial tag-encoded FLX amplicon pyrosequencing (bTEFAP) and data analysis

To characterize the microbial community associated with *C. rubiginosa*, 20 adults (ten males and ten females) were submerged in liquid nitrogen and crushed with sterile pestles. DNA was extracted using the QIAGEN DNeasy Blood & Tissue Kit (Hilden, Germany) according to the manufacturer's instructions. DNA concentrations were calibrated to 50 ng/μl and subsequently pooled into a single sample. BTEFAP was performed using an external service provider, MR DNA Laboratory (Lubbock, TX, USA), with 16S rRNA primers Gray 28F and Gray 519R (Sun et al., 2011). A sequencing library was generated through one-step PCR with 30 cycles, using a mixture of Hot Start and HotStar high fidelity *Taq* polymerases (QIAGEN). Sequencing extended from Gray28F, using a Roche 454 FLX instrument with Titanium reagents and procedures. Low quality reads (quality cutoff = 25) and sequences < 200 bp were removed following sequencing. Analysis of high-quality reads was conducted using QIIME (Caporaso et al., 2010). Briefly, we retained sequences between 200 and 600 bp in length, allowing no errors in the barcode but one mismatch in the primer and one ambiguous base. The minimum average quality score per read was set to 25, and reads that were not assigned to any barcode were discarded. Closed-reference OTU picking was performed with the algorithm *cdhit* (QIIME) using 97% similarity as a threshold to cluster the sequences into OTUs (Berasategui et al., 2016).

Phylogenetic analysis

Curated, full symbiont 16S rRNA sequences were aligned using the program SeaView (Gouy et al., 2010), and phylogenetic relationships were reconstructed using the maximum likelihood algorithm as implemented in MEGA 7 (Kumar et al., 2016) according to the Tamura-Nei (G + I) model. Bootstrap values for nodes were computed based on 2,000 resamples.

Diagnostic PCR screening

Using 102 *C. rubiginosa* adults collected from separate populations across New Zealand, the United States, Germany and Japan, we screened for the presence of *Stammera* and *Wolbachia*. Specific primers were utilized to detect either of the two dominant symbionts using diagnostic PCR reactions. PCR amplifications were conducted on a VWR Gradient Thermocycler (Radnor, PA, USA) using 12.5 μl reactions, including 1 μl of DNA template, 1X PCR buffer [20 mM Tris-HCl, 16 mM $(NH_4)_2SO_4$, and 0.01% Tween 20], 2.5 mM $MgCl_2$, 240 μM dNTPs, 0.8 μM of each primer, and 0.5 U of Taq DNA polymerase (VWR, Radnor, PA, USA). The following

cycle parameters were used: 3 min at 94°C, followed by 32 cycles of 94°C for 40 s, 68/66°C for 1 min (*Stammera*/*Wolbachia* primers respectively), and 72°C for 1 min, and a final extension time of 4 min at 72°C.

Symbiont localization by fluorescence *in situ* hybridization (FISH)

To localize *Stammera* within its host, we employed FISH on whole-mount as well as semithin section preparations as previously described by Weiss and Kaltenpoth (2016). A specific oligonucleotide probe Cy5_StammeraF was designed using the bacterium's 16 rRNA sequence. A single dissection from an ovipositing female including the foregut, midgut, hindgut, and ovaries was washed three times using 0.3% Triton X-100 in PBS prior to whole-mount FISH. The tissue was permeabilized in 70% acetic acid for 1 min at 60°C, followed by a 30 min incubation in hybridization buffer (0.9 M NaCl, 0.02 M Tris/HCl pH 8.0, 0.01% SDS) at 60°C. The sample was then incubated at 60°C for 16 h in 100 μl hybridization buffer containing 5 μl of the symbiont-specific probe Stammera_Cy5 (500 nM) as well as 5 μg/ml DAPI for counterstaining of host cell nuclei. Washing was accomplished by inundating the sample in wash buffer (0.1 M NaCl, 0.02 M Tris/HCl pH8.0, 0.01% SDS, 5 mM EDTA) for 2 h at 60°C, and twice in dH_2O for 30 min at 60°C. The tissues were mounted on a microscope slide, then embedded in VectaShield (Vector, Burlingame, CA, USA). Images were generated using a Zeiss AxioImager.Z1 fluorescence microscope (Jena, Germany).

For higher resolution of symbiont-bearing structures within the gut, accessory reproductive glands and eggs, FISH was also performed using semithin sections of *C. rubiginosa*. Samples were embedded in Technovit 8100 (Heraeus Kulzer, Wehrheim, Germany), and semithin sections (8 μm) were generated on a microtome (Microm HM355S) using a glass blade. Sections were subsequently transferred to silanized microscope slides (Marienfeld) and subjected to hybridization for 90 min at 60°C using the aforementioned hybridization mixture. Slides were washed using warm washing buffer (composition as above), then rinsed with dH_2O. Upon drying at room temperature, VectaShield was applied prior to observation under the fluorescence microscope.

3D-reconstruction of symbiont-bearing egg caplets

For three-dimensional reconstruction of the symbiont transmission structure, an egg clutch was fixated in Bouin solution at 4 °C, dehydrated in a graded ethanol series and in isopropanol and embedded using the Epoxy Embedding Medium kit (Sigma-Aldrich, Germany) two days after oviposition. Semithin sections (2 μm) were then produced using a microtome (Microm HM355S) with a diamond blade and transferred to silanized microscope slides. Samples were stained with a filtered toluidine blue/pyrimidine solution (0.4% toluidine blue, 0.1% pyrimidine G and 0.4% di-sodium-tetraborate in water) for 2 min at 60°C, washed briefly in water, air-dried, treated briefly with xylol, and then embedded in Entellan (Merck). Images of all sections were acquired on an AxioImager.Z1 and aligned with Fiji. For this, a TrakEM2 and an automatic alignment was generated. This dataset was loaded into Amira 5.4.1 (Fei, Hillsboro, OR, USA) for 3D reconstruction.

Quantitative PCR

Symbiont titers across host development were estimated via quantitative PCR (qPCR) using a RotorGene-Q cycler (QIAGEN, Hilden, Germany) with DNA extracts from eggs, larvae (1^{st}, 3^{rd}, 5^{th} instars), pupae, and adults (pre- and post-diapause). The final reaction volume of 25 μl included the following components: 1 μl of DNA template, 2.5 μl of each primer (10 mM), 6.5 μl of autoclaved distilled H_2O and 12.5 μl of SYBR Green Mix (QIAGEN, Hilden, Germany). The primers used were specific for the 16S rRNA gene of *Stammera* (Stammera_F/Stammera_R2; Key Resources Table). Verification of primer specificity was conducted *in silico* by comparison with reference sequences of all known bacterial taxa in The Ribosomal Database (https://rdp.cme.msu.edu). Additionally, PCR products were sequenced to confirm primer specificity *in vitro*. Conditions for qPCR were optimized using a VWR Gradient Thermocycler (VWR, Radnor, PA, USA) at various annealing temperatures (60-68°C). Standard curves (10-fold dilution series from 1 to 10^{-6} ng/μl) were generated using purified PCR products and measuring their DNA concentration using a NanoDropTM1000 spectrophotometer (Peqlab). For qPCR, the following cycling parameters were used: 95°C for 10 min, followed by 45 cycles of 68°C for 30 s, 72°C for 20 s and 95°C for 15 s. Subsequently, a melting curve analysis was conducted by increasing the temperature from 60°C to 95°C within 20 min. Based on the standard curve, absolute copy numbers of specific 16S templates were calculated, which were then used to extrapolate symbiont population size by accounting for the single copy of the 16S gene in *Stammera*'s genome.

Experimental manipulation of the symbiont-bearing egg caplet

13 egg clutches (5-8 eggs each) from different *C. rubiginosa* females were harvested two days following oviposition. Eggs were then separated into three experimental treatments: (i) egg caplet pierced, sterilized; (ii) egg caplet not pierced, sterilized; (iii) untreated control.

For treatment (i), egg caplets were punctured using sterile dissection pins (Movie S1), then prodded with the loophole-end of a needle that had been inundated in 95% ethanol. To ensure that developmental and survival effects observed in treatment (i) were not simply a consequence of ethanol exposure, egg caplets that were not punctured were also prodded with needles inundated with 95% ethanol, resulting in treatment (ii) – serving as an additional control group to the untreated treatment (iii). Individuals across all experimental groups were observed on a daily basis for the assessment of fitness effects across the different groups. Survival until adulthood was recorded. All experimental individuals were subjected to *Stammera*-specific diagnostic PCR (Stammera_F/Stammera_R2; Key Resources Table), including surviving adults as well as deceased larvae.

Symbiont genome sequencing, assembly, and annotation

DNA was purified, as described above, from 10 symbiotic organs extracted from five adult *C. rubiginosa*. Sequencing was performed at the Max Planck Genome Centre Cologne on the HiSeq 2500 Sequencing System from Illumina (https://www.illumina.com/webcite), utilizing the paired-end 100 bp technology and at a depth of ~12 million reads. Adaptor sequences were trimmed with Trimmomatic v0.03 using the default parameters (Bolger et al., 2014). To filter beetle-, plant-, and *Wolbachia*-associated sequences, the quality controlled reads were mapped using Bowtie2 (Langmead and Salzberg, 2012) to the publicly available sequences of closely related species. Assembly was performed using Spades under default parameters (Bankevich et al., 2012). This resulted in ~400 thousand contigs. After assembly, the contigs were screened for GC content and taxonomic identity to Enterobacteriacea via BLAST to filter out remaining contaminant sequences. In total, 11 contigs were then further assembled into scaffolds using GapFiller (Boetzer and Pirovano, 2012). The four resulting genomic scaffolds were subsequently connected and circularized by PCR and Sanger sequencing. The final genome sequence was automatically annotated using RAST (Aziz et al., 2008) according to the genetic code 4 (TGA encoding tryptophan) to computationally translate the predicted protein-coding genes.

Transcriptome sequencing, assembly, and annotation and PCWDE identification

Three *C. rubiginosa* adults were dissected on an RNaseZap-treated (Sigma-Aldrich, St. Louis, MO, USA) plate and both pairs of foregut symbiotic organs were then freed from the rest of the insect's body. The symbiotic organs, as well as their respective symbiotic organ-free whole beetles were immediately subject to RNA extraction using the QIAGEN RNA Extraction kit (Hilden, Gemany) according to the manufacturer's instructions. Sequencing of the resulting six samples (3X symbiotic organs; 3X whole insects) was performed at the Max Planck Genome Centre Cologne on the HiSeq 2500 Sequencing System from Illumina (https://www.illumina.com/webcite), utilizing the paired-end 100 bp technology at a depth of 100 million reads.

Quality control measures including filtering high-quality reads based on the fastq score, trimming the read lengths. *De novo* transcriptome assemblies were carried out using CLC Genomics Workbench v10.0.1 (https://www.qiagenbioinformatics.com/products/clc-genomics-workbench/). Selecting the presumed optimal consensus transcriptome as well as subsequent transcriptome annotation using BLAST and Gene Ontology were done as described previously (Jacobs et al., 2016; Vogel et al., 2014). In brief, three assemblies were generated for each dataset, with standard settings and two additional CLC-based assemblies with the following parameters: word size = 64 (automatic); bubble size = 250 (automatic); scaffolding option selected; reads were mapped back to contigs with the following alternative options: nucleotide mismatch cost = 1(2); insertion = deletion costs = 2(3); length fraction = 0.5(0.7); similarity = 0.9(0.85). Conflicts among individual bases were resolved in all assemblies by voting for the base with the highest frequency. Contigs shorter than 250 bp were removed from the final analysis. The three assemblies were compared according to quality criteria such as N50 contig size, total number of contigs and the number of sequence reads not included in the contig assembly. The *de novo* reference transcriptome assembly contig sequences were used to search the NCBI nr nucleotide database with the blastall program. Homology searches (BLASTx and BLASTn), and functional annotation according to GO terms (http://www.geneontology.org) and enzyme classification (EC) codes were carried out using Blast2GO PRO v4.1.5 (https://www.blast2go.com;(Götz et al., 2008)) as previously described (Vogel et al., 2014). The *de novo* reference transcriptome of *C. rubiginosa* symbiotic organs was assembled using 200 Mio sequence reads and contained 143,623 contigs (minimum contig size = 250 bp) with an N50 contig size of 712 bp and a maximum contig length of 27,590 bp. The *C. rubiginosa* whole body transcriptome assembly using 67 Mio sequence reads contained 153,298 contigs with an N50 contig size of 781 bp and a maximum contig length of 19,057 bp.

In addition to global homology searches, functional annotation, and enzyme classification, contigs corresponding to plant cell wall degrading enzymes (PCWDEs) were retrieved from the above described transcriptomes by BLAST-searches using all publically available as well as in-house PCWDE sequences from insects, nematodes, bacteria, and fungi as queries. We performed a separate BLAST by groups of species to increase the sensitivity of the search.

Heterologous pectinase expression and purification

Pectinase-coding genes of interest, PG and RL, were synthesized using Genscript (Piscataway, NJ, USA), including codon optimization for expression in *E. coli,* and were subsequently cloned into pET-22b(+). Plasmids were transformed into BL21 Star (DE3) and clones were picked for heterologous expression using the Overnight Express Autoinduction System 1 by Novagen according to the protocol (Merck, Kenilworth, NJ, USA). Specifically, 5 mL starter cultures in Lysogeny Broth containing 100μg/ml ampicillin were incubated at 18°C and 220rpm until log phase (OD_{600} = 0.5-1.0) in 50 mL conical tubes. Aliquots of starter cultures were then centrifuged at 1000 x g for 5 min, the medium was removed and cell pellets were re-suspended in autoinduction medium. Re-suspended cells were used to inoculate main cultures to OD_{600} = 0.01. Autoinduction cultures were incubated in baffled flasks (50ml medium/250ml flask) at 18°C and 200rpm for 40h. Cells were pelleted and subsequently lysed with Novagen BugBuster 10x (Merck, Kenilworth, NJ, USA) in Immobilized Metal Affinity Chromatography (IMAC) Binding buffer (see below) supplemented with Lysonase by rotating the samples at room temperature for 30 min. Samples were centrifuged and the supernatant was subjected to IMAC purification on a column self-packed with 1 mL HisPur cobalt resin. After applying samples in IMAC Binding buffer (50 mM sodium phosphate buffer pH 7.7, 0.5M sodium chloride, protease inhibitor) on the pre-equilibrated column, the resin was washed extensively (50 mM sodium phosphate buffer pH 7.7, 0.3M sodium chloride, 10mM imidazole, protease inhibitor) and eluted three times (sodium phosphate buffer pH 7.4, 0.3M imidazole, protease inhibitor) with 1min. incubation time for each elution step. Elution fractions were desalted against water on Zeba Spin Desalting columns with a 7 kDa cutoff (Thermo Scientific) and used for enzymatic assays.

Success of expression and purification was monitored by western blot using an Anti-His (C-term)-HRP Antibody and the SuperSignal West HisProbe Kit (both Thermo Scientific).

Whereas the PG expression was successful, rhamnogalacturonan lyase expression failed even after testing with different expression conditions, vectors, and various cell lines. In detail, the Overnight Express Autoinduction System 1 (Novagen, Merck, Kenilworth, NJ, USA) as well as IPTG based induction was used for expression in the *E. coli* strains BL21 Star (DE3), BL21 Star (DE3)pLysS (both Thermo Scientific, Waltham, MA, USA), NiCo21 (DE3) (NEB) and RV308 (provided by Dr. C. Haupt, Ulm Germany) at 18°C to 37°C in pET-22b(+) for potential periplasmic and pET101/D-TOPO (Thermo Scientific, Waltham, MA, USA) for cytosolic localization. Expression of the RL open reading frame inserted into pET-22b(+) and pET101/D-TOPO, transformed into DE3 and K-12 RV308 *E. coli* strains was performed as described above. In case of IPTG based induction of expression, starter cultures were used to inoculate main cultures at a 1:100 dilution. Main cultures were subsequently incubated at 37°C and 220rpm until OD_{600} = 0.5. Expression was induced with 0.1 mM or 0.5 mM IPTG at 37°C, 30°C, 23°C or 18°C and 200rpm for 3h to 40h. Cells were pelleted and lysed as described above and supernatants as well as pellets were directly subjected to western blot analysis for monitoring success of expression. In addition, expression was also tested transiently in *Spodoptera frugiperda* ovarian tissue (SF9) insect cells grown in Sf-900 II serum free medium containing 50μg/ml Gentamycin at 27°C (both Thermo Scientific) after transfection of a rhamnogalacturonan lyase open reading frame in pMIB/V5-His (Thermo Scientific) using FuGENE HD transfection reagent (Promega). Proteins were harvested after 72h transient expression in 6-well Multiwell plates for cell culture (Thermo Scientific) and culture medium as well as cell pellets were subjected to western blot using an Anti-V5-HRP Antibody to test for expression success. In all cases pET-22b(+)_GH28 or pMIB/V5-His_GH28 were used as positive controls, respectively. In none of these expression attempts was a rhamnogalacturonan lyase signal obtained by western blot.

Spodoptera frugiperda ovarian tissue (SF9) insect cells as well as all bacterial cell lines, except for K-12 RV308, were purchased from well-established companies. Thus, the cell lines used herein have not been authenticated in our lab. The K-12 RV308, provided by Dr. C. Haupt, originated from ATCC.

Enzymatic assays

Agarose diffusion assays were performed in 1% agarose Petri dishes containing either 0.1% polygalacturonic acid, rhamnogalacturonan I (both Megazyme) or 0.1% carboxymethylcellulose (CMC) and 50 mM citrate/phosphate buffer pH 5.0. Two millimeter holes were made into the agarose, and samples were loaded in 5 μL steps. Activity was revealed after 2 h of incubation at room temperature with 0.1% Ruthenium red solution (polygalacturonic acid, rhamnogalacturonan I) or 1 h of incubation at 30°C with 0.1% Congo Red solution (for carboxymethylcellulose). Plates were then destained with distilled water until pale activity zones appeared against a dark red background. Qualitative analysis of breakdown products was performed by thin layer chromatography (TLC) of 20 μl enzyme assays set up as follows: 14 μl of recombinant PG or crude gut extract of symbiotic and aposymbiotic *Cassida rubiginosa* larvae were incubated with either 0.2% polygalacturonic acid or rhamnogalacturonan I in 20 mM citrate/phosphate buffer pH 5.0 at 40°C for about 16 h. The whole assay volumes were used for TLC afterward. In detail, samples were applied to TLC plates (Silica gel 60, 20 × 20 cm, Merck) in 4 μl steps and plates were developed ascending with ethyl acetate:glacial acetic acid:formic acid:water (9:3:1:4) for about 60 min. After drying, carbohydrates were stained by spraying the plates with a solution containing 0.2% (w/v) orcinol in methanol:sulfuric acid (9:1), followed by a short heating until spots appeared. The reference standard contained 2 μg each of galacturonic, di-galacturonic, tri-galacturonic acid and rhamnose. In quantifying the symbiont's recombinant PG hydrolytic activity across a variety of methylated pectic substrates, 3,5-dinitrosalicylic acid (DNS) assays were additionally performed to measure the release of galacturonic acid equivalents. Assays were set up like those for TLC but scaled up from 20 μl to 60 μl. In detail, 21 μl of recombinant PG was incubated with 0.2% of either demethylated polygalacturonic acid, pectin from citrus peel or esterified pectin from citrus fruit (Sigma) in a 20 mM citrate/phosphate buffer pH 5.0 at 40°C for 16 h. As a negative control, the PG enzyme was boiled before incubation. Each assay was set up in three replicates. The reducing groups released after pectin hydrolysis were quantified by the DNS method (Miller, 1959) with slight modifications. Three solutions were prepared for analysis of these samples in advance as follows: solution 1 containing DNS, phenol and sodium hydroxide to a final concentration of 0.1%, 0.2% and 1% (w/v) in water respectively. Solution 2 is a 100-fold stock of sodium sulfite to a final concentration of 0.5% (w/v) in water and solution 3 is a 7-fold stock of potassium sodium tartrate (Rochelle salt) to a final concentration of 40% (w/v) in water. A mixture of solution 1 and 2 in a 99:1 ratio (v/v) was prepared fresh each time just before use, added to a sample to be analyzed in a 1:1 ratio (v/v) followed by heating for 5 min in a PCR cycler at 99°C. Solution 3 was added in a 1:6 ratio (v/v) and the whole mixture was cooled down to room temperature before reading the absorbance at 575 nm on an Infinite M200 microplate reader (Tecan). The amount of reducing acids released was calculated based on a galacturonic acid standard curve.

Immunohistochemistry

The digestive tract of adult females were isolated in PBS and fixed with PBS containing 4% formaldehyde at 4°C overnight. After several washes with PBS, the foregut-midgut junction with the symbiotic organs was isolated in PBS and then embedded in Technovit 8100 (Kulzer, Germany) according to the manufacturer's protocol. Tissue sections of 3 μm in thickness were prepared by using a rotary microtome RM2165 (Leica, Germany) and mounted on hydrophilic-coated glass slides (Matsunami, Japan). The sections were treated with methanol containing 1% H_2O_2 at room temperature for 15 min to inactivate indigenous peroxidase. After several washes with PBS, sections were incubated in PBS-10% normal goat serum containing the anti-pectinase antibody at

room temperature. After overnight incubation, the sections were washed with PBS at room temperature for 5 min three times, and incubated in PBS-10% normal goat serum containing the anti-rabbit IgG goat antibody conjugated with peroxidase (Sigma-Aldrich, USA) at room temperature for 30 min. Then, the sections were washed with PBS at room temperature for 5 min three times. Signals were detected as infrared fluorescence of Cy5 using TSA-Plus Cyanine 3/Cyanine 5 System (PerkinElmer, USA) according to the manufacturer's protocol. After several washes with H_2O, the sections were counter-stained with DAPI and mounted in SlowFade Gold antifade reagent (Thermo Fisher Scientific, USA). The mounted sections were observed under the epifluorescence microscope Imager.Z2m equipped with the digital camera AxioCam MRm (Carl Zeiss, Jena, Germany). The obtained images were merged and adjusted using Zen2 blue edition (Carl Zeiss, Jena, Germany).

QUANTIFICATION AND STATISTICAL ANALYSIS

C. rubigionsa survivorship until adulthood were compared across the three experimental treatments using the Kaplan-Meier, Tarone-Ware test as implemented in the SPSS 17.0 software package (SPSS, Chicago, IL, USA). In Figure 2C, n (39) refers to the number of larvae spread evenly (13 each) across the three treatments as outlined in Table S2. To compare pectinase expression dynamics between the foregut symbiotic organs relative to the whole body based on PG and RL transcripts per million (Figure 3G), an ANOVA was performed in SPSS 17.0 (SPSS, Chicago, IL, USA). The following definitions of significance are shown in the respective figures: $*p < 0.05$ for the Kaplan-Meier, Tarone-Ware test (Figure 2C), and $***p < 0.0001$ for ANOVA (Figure 3G).

DATA AND SOFTWARE AVAILABILITY

The accession number for the *Stammera* genome reported in this paper is GenBank: CP024013, based on the Bioproject identification number PRJNA413589. The accession number for the transcriptome data reported in this paper is GenBank Bioproject: PRJNA414435. The accession number for the 454 pyrosequencing data (raw sff files) reported in this paper is NCBI SRA: SRP119423.

Cell

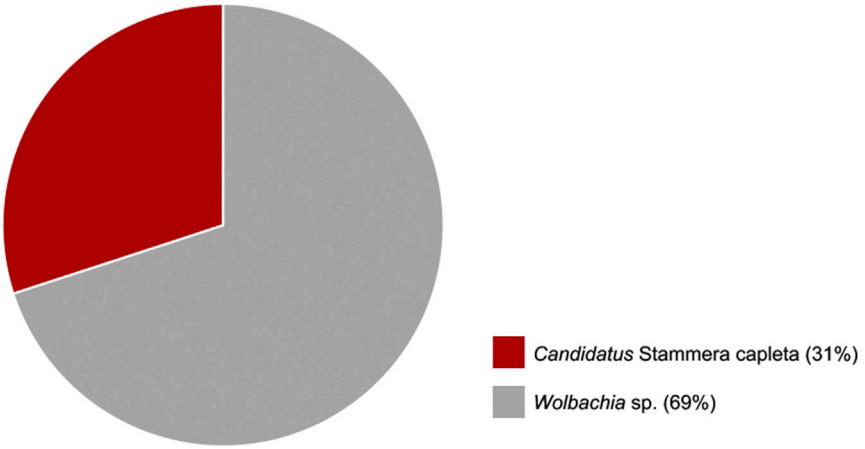

Figure S1. Bacterial Community Composition of *Cassida rubiginosa* Adults, as Revealed by Bacterial 16S rRNA Tag-Encoded FLX Amplicon Sequencing, Related to the STAR Methods

bTEFAP and data analysis. Chart represents a pooled sample of 20 individuals (ten males and ten females) collected in Lincoln, New Zealand.

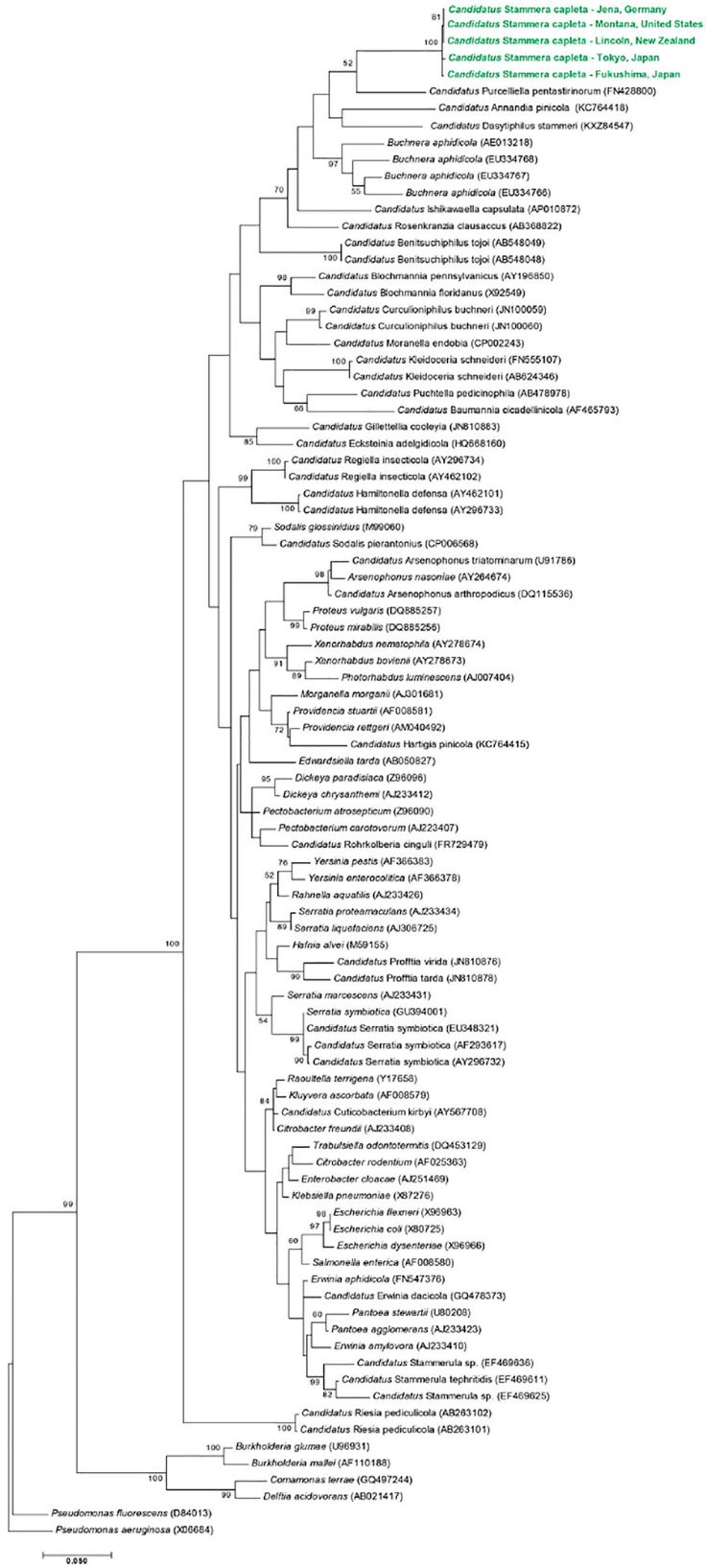

(legend on next page)

Figure S2. Phylogenetic Affiliation of "*Candidatus* Stammera capleta" (in Green) within the Enterobacteriaceae, Based on Complete 16S rRNA Sequences, Related to the STAR Methods

Phylogenetic relationships were constructed with an approximately maximum-likelihood algorithm as implemented in MEGA using the Tamura-Nei (G + I) model. The tree with the highest log likelihood (−13895.0490) is shown. Bootstrap support values from 2,000 resamples are given at the nodes.

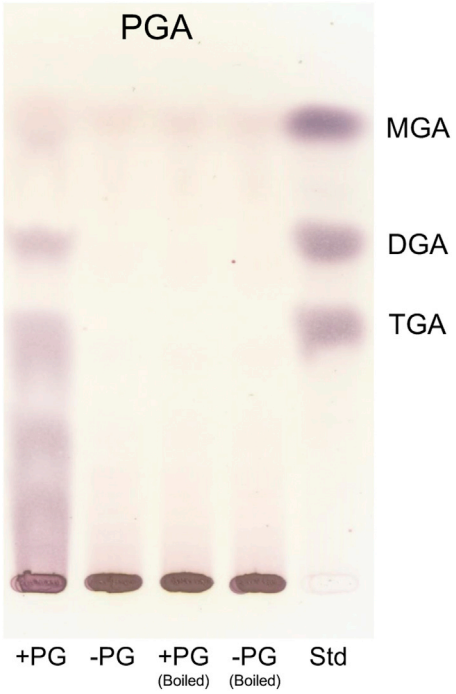

Figure S3. Thin-Layer Chromatogram of +PG and -PG Activity Assays against PGA, as well as Boiled Controls, +PG (Boiled) and -PG (Boiled), Related to Figure 4B

Standard (Std); mono-galacturonic acid (MGA); di-galacturonic acid (DGA); tri-galacturonic acid (TGA).

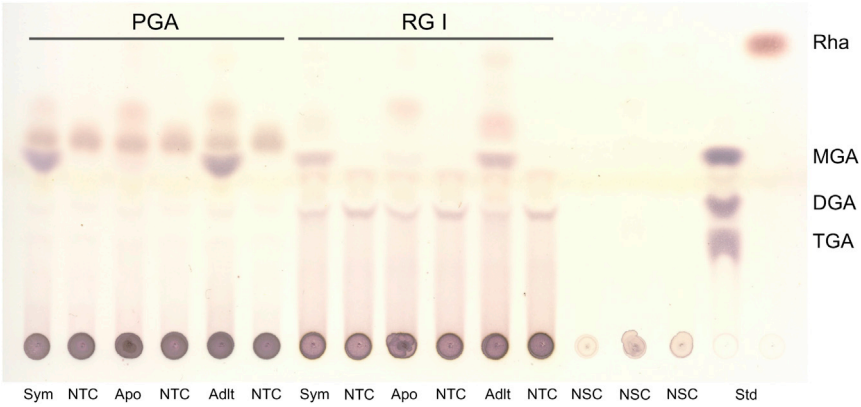

Figure S4. Thin-Layer Chromatogram Illustrating Breakdown Products Of Pectinase Activity In Symbiotic (Sym) and Aposymbiotic (Apo) Larvae, as well as a No Template Control (NTC), Symbiotic Adult (Adlt) against PGA and RG I, Related to Figure 5B

No substrate controls (NSC) were included. Standard (Std.); mono-galacturonic acid (MGA); di-galacturonic acid (DGA); tri-galacturonic acid (TGA) and rhamnose (Rha).

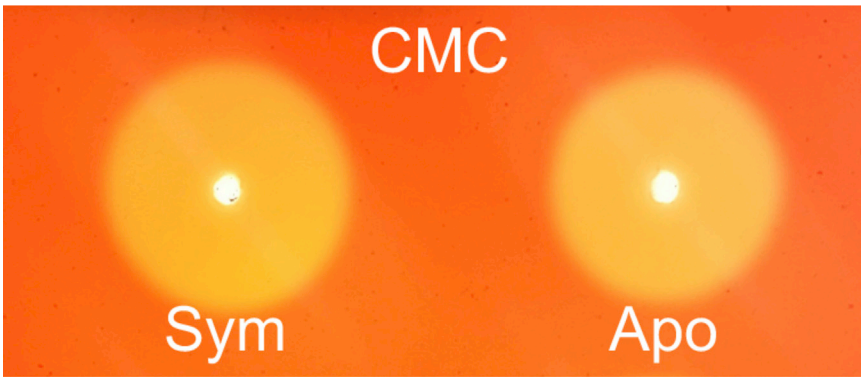

Figure S5. Cellulolytic Capacity in *Cassida rubiginosa* following Symbiont Manipulation, Related to the STAR Methods

Agarose diffusion assays depicting cellulase activity in symbiotic (Sym) and aposymbiotic (Apo) larvae using gut protein extracts following application to gels containing carboxymethylcellulose (CMC).